# Description and evaluation of a surface runoff susceptibility mapping method

L.R. Lagadec, Pierre Patrice, Isabelle Braud, B. Chazelle, L. Moulin, J. Dehotin, E. Hauchard, Pascal Breil

1     **Special Issue of Journal of Hydrology:**

2     SI: Flash Floods and Landslides

3

4     **Title:**

5     Description and evaluation of a surface runoff susceptibility mapping method

6

7     **Authors:**

8     Lilly-Rose Lagadec[1,2,*], Pierre Patrice[2], Isabelle Braud[2], Blandine Chazelle.[1], Loïc Moulin[1], Judicaël

9     Dehotin[1], Emmanuel Hauchard[3], Pascal Breil[2]

10     Affiliations:

11     [1] SNCF Réseau, Engineering and Project Direction, 6 avenue François Mitterrand, 93574, La Plaine

12     Saint Denis, France.

13     [2] IRSTEA, HHLY, Hydrology-Hydraulic Department, Centre de Lyon-Villeurbanne, 5 rue de la Doua,

14     69626 Villeurbanne, France.

15     [3] Agglomeration community of Le Havre (CODAH), 19 rue Georges Braque 76085 Le Havre Cedex,

16     France / UMR M2C 6143 CNRS Geology Department University of Rouen, France

17     Correspondence to: Lilly-Rose Lagadec (lrlagadec@gmail.com)

18

**Abstract**

21    Surface runoff is the hydrological process at the origin of phenomena such as soil erosion, floods out

22    of rivers, mudflows, debris flows and can generate major damage. This paper presents a method to

23    create maps of surface runoff susceptibility. The method, called IRIP (Indicator of Intense Pluvial

24    Runoff, French acronym), uses a combination of landscape factors to create three maps representing

25    the susceptibility (1) to generate, (2) to transfer, and (3) to accumulate surface runoff. The method

26    input data are the topography, the land use and the soil type. The method aims to be simple to

27    implement and robust for any type of study area, with no requirement for calibration or specific

28    input format. In a second part, the paper focuses on the evaluation of the surface runoff

29    susceptibility maps. The method is applied in the Lézarde catchment (210 km², northern France) and

30    the susceptibility maps are evaluated by comparison with two risk regulatory zonings of surface

31    runoff and soil erosion, and two databases of surface runoff impacts on roads and railways.

32    Comparison tests are performed using a standard verification method for dichotomous forecasting

33    along with five verification indicators: accuracy, bias, success ratio, probability of detection, and false

34    alarm ratio. The evaluation shows that the susceptibility map of surface runoff accumulation is able

35    to identify the concentrated surface runoff flows and that the susceptibility map of transfer is able to

36    identify areas that are susceptible to soil erosion. Concerning the ability of the IRIP method to detect

37    sections of the transportation network susceptible to be impacted by surface runoff, the evaluation

38    tests show promising probabilities of detection (73 to 90%) but also high false alarm ratios (77 to

39    92%). However, a qualitative analysis of the local configuration of the infrastructure shows that

40    taking into account the transportation network vulnerability can explain numerous false alarms. This

41    paper shows that the IRIP method can be a valuable tool to facilitate field analysis and perform

42    surface runoff zonings and opens interesting prospects for the use of the IRIP method in a context of

43    risk management.

44      ## 1.  Introduction

45      Intense surface water runoff is a hydrological process which can generate major damage. When the

46      surface water concentrates, it gains enough energy to erode soil particles, which makes the water

47      denser and more powerful (Wischmeier, 1959). Intense surface runoff includes phenomena such as

48      soil erosion, floods out of river networks, mudflows, and debris flows. According to the Gaspar

49      French database[1], which collects information on natural disasters at a district level, around 40% of

50      flood damage is due to intense surface runoff in France (Dehotin and Breil, 2011a). Surface runoff

51      often impacts populations and infrastructures such as homes or transportation networks (Chazelle et

52      al., 2014). The environment can also be impacted by surface runoff through soil loss and the transfer

53      of pollutants contained in soils.

54      For this study, surface runoff is defined as water from precipitation which does not infiltrate into the

55      soil and flows on the surface until it reaches a permanent river. This hydrological process can also be

56      called overland flow (Hewlett, 1982). Two surface-runoff generation processes can be distinguished:

57      infiltration excess overland flow, when the rain intensity is higher than the soil infiltration capacity,

58      called hortonian runoff (Horton, 1933); and saturation overland flow, when soil storage capacity is

59      limited or the soil is already saturated (Hewlett and Hibbert, 1967). These processes are difficult to

60      observe in the field because they occur quickly and they can occur simultaneously (Cros-Cayot,

61      1996). In general terms, surface runoff is a difficult-to-measure phenomenon (Dehotin et al., 2015).

62      Once surface water flows downstream, it can infiltrate, be transferred or be accumulated –

63      depending on topographical and micro-topographical features – or join a watercourse or drainage

64      system. Surface runoff can flow in a diffuse or concentrated manner. Many factors can influence or

65      reduce surface runoff in a catchment: soil characteristics (type, thickness, roughness, permeability)

66      (Piney, 2009), initial water content, land use (vegetation, urbanization, agricultural land), geology

67      (Onda et al., 2001), topography, geomorphology (ability to concentrate, plateau/valleys distribution)

68      (Douvinet et al., 2008), and rainfall characteristics (intensity, frequency, duration) (Galevski, 1955).

69      In the field of risk management, some terms can have a wide range of definitions, depending on the

70      field of application (Christensen et al., 2003; Thywissen, 2006). The following definitions are retained.

71      Firstly, intense surface runoff is a natural hazard, which means a natural event, potentially

72      dangerous, occurring randomly in space and time (UNDRO, 1979). Risks induced by intense surface

73      runoff are impacts that surface runoff may potentially cause to society (people, goods, environment,

74      economy, etc.). A risk is the combination of a hazard and a vulnerability (UNDHA, 1992). Vulnerability

---

[1] https://www.data.gouv.fr/fr/datasets/gaspar/

75    is often defined as a measure to assess the quantity of loss potentially generated by a hazard (Buckle

76    et al., 2000; Society for Risk Analysis, 2015). In this study, the vulnerability of the transportation

77    network refers to its structural vulnerability; the higher the vulnerability, the higher the possibility of

78    being physically damaged.

79    In the scientific literature, there are many models for the simulation or mapping of surface runoff

80    processes. They may be classified into various approaches: naturalistic, topographic, a combination

81    of criteria or hydrological modeling. Naturalistic approaches often provide results consistent with the

82    reality but they require a very good understanding of the study area, can be applied to rather small

83    areas, and are difficult to replicate (Abudi et al., 2012; Dehotin et al., 2015a; Holzmann and Sereinig,

84    1997; Tetzlaff et al., 2007). Topographical approaches using information from Digital Elevation

85    Models (Delahaye et al., 2002; Langlois and Delahaye, 2002; Pons et al., 2010) have the advantage of

86    being simple and can be automated but the mapping of surface runoff needs to take into account

87    many other parameters such as land use or soil type. Criteria combination approaches also remain

88    relatively straightforward while taking into account multiple parameters. The review of existing

89    methods reveals that most of them focus on water erosion or landslide (Akgun and Türk, 2010;

90    Faulkner et al., 2010; Guillobez et al., 2000; Le Bissonnais et al., 2002; Schmocker-Fackel et al., 2007).

91    Hydrological modeling techniques are both accurate and provide quantitative results including the

92    time evolution of the processes (Carpenter et al., 1999; Cerdan et al., 2002; Dabney et al., 2011;

93    DeRoo et al., 1996; Laflen et al., 1991; Smith et al., 1995). Some are extremely complex. They require

94    significant computational time, calibration to be applied to different catchments, and a large quantity

95    of data. This rapid overview shows that there are multiple methods for surface runoff mapping but

96    the maps are either difficult to reproduce automatically, need many complex input data, or the

97    method is focused on a specific phase of the phenomenon (the accumulation areas, the low

98    infiltration areas or the erosion areas) and do not address all the aspects of the entire runoff process.

99    For this reason, a method called IRIP for Indicator of Intense Pluvial Runoff (French acronym) has

100    been developed to produce comprehensive mapping of areas susceptible to generate, to transfer,

101    and to accumulate surface runoff without explicit hydrological modeling and using open access data

102    (Dehotin et al., 2015a; Dehotin and Breil, 2011a). This automatic method can be applied to a large

103    range of study area sizes with data at various resolutions. However, the validity and relevance of the

104    produced maps must be evaluated carefully and rigorously.

105    The evaluation of hazard models is an important step in model developments. Indeed, model outputs

106    can be used for stakeholder decision-making in risk management. The stakes are very high (cost of

107    structural and organizational adjustments, safety risks) and wrong decisions can lead to serious

108    consequences. It is essential to know the exact value of model outputs, that is, the assumptions

109    made, the application range, and uncertainties related to the results. Globally, model evaluation

110    suffers from a lack of methodological guidelines (Moriasi et al., 2007). For surface runoff hazard

111    models, the evaluation is particularly complex because of the lack of surface runoff data. The

112    phenomenon rapidity and scarcity make large-scale observation and instrumentation a complex issue

113    (Dehotin et al., 2015a; Hudson, 1993). The IRIP method has already undergone numerous evaluations

114    using in-situ measurements (Dehotin et al., 2015a; Laverne, 2013) and discharge data (Arnaud and

115    Dehotin, 2011; Legros, 2014) but to go further in the evaluation procedure and to assess the

116    relevance of the IRIP method from the point of view of risk assessment, the use of proxy data is

117    suggested. Proxy data are data which are not direct measurements of the phenomenon but are

118    related to it and provide large-scale evidence of the phenomenon occurrence (IPCC, 2003). Some

119    studies in hydrology use proxy data to evaluate models, such as flooded road reports (Naulin et al.,

120    2013; Versini et al., 2010a, 2010b), observations of gravitational hazards in mountainous areas

121    (Defrance, 2014), and post-event surveys (Javelle et al., 2014; Ortega et al., 2009). Concerning the

122    IRIP method evaluation, few comparisons have been performed with proxy data such as surface

123    runoff impact locations on railways (Dehotin et al., 2015b) and natural disaster declaration locations

124    from the Gaspar French database (Dehotin and Breil, 2011a). However, these tests have been

125    performed for few case studies and remain qualitative. Indeed, the comparison between model

126    outputs and proxy data generates technical issues: for example, how can data that are different in

127    form and content and that do not carry the same information be compared reliably? The use of proxy

128    data highlights the lack of methodological framework but also shows the valuable contribution of this

129    type of data for model evaluation.

130    The first objective of this paper is to present the IRIP method for surface runoff susceptibility

131    mapping. The second objective is to evaluate the IRIP maps by comparison with different types of

132    proxy data available on the study area: regulatory zonings of surface runoff and soil erosion and

133    databases of surface runoff impacts on roads and railways. The paper proposes an evaluation

134    method that allows quantitative evaluation of the spatial information contained in the IRIP maps.

135    Finally, development paths are discussed to adapt the IRIP method as a tool for risk management.

### 2.   Materials and Methods

### 2.1. The IRIP Method

138    IRIP is a method to map the spatial distribution of areas susceptible to surface runoff. The IRIP

139    method concept is based on the creation of three susceptibility maps which represent surface runoff

140    generation, transfer, and accumulation. Note that, to obtain a hazard map, the rainfall must be taken

141    into account and to get a risk map, the hazard map must be combined with the stakes of the study

142    area and their vulnerabilities. These two aspects are not considered in the present study, which only

143    focuses on the susceptibility maps provided by the IRIP method.

144    Each susceptibility map (generation, transfer, and accumulation) is created by combining five

145    indicators, summarised in Table 1 (columns 1&2). Each indicator is classified in two categories

146    favourable (1) or not favourable (0) to surface runoff (Table 1, col 3), providing a binary map. The five

147    maps are subsequently assembled to produce a surface runoff susceptibility map from 0 (not

148    susceptible) to 5 (very susceptible). This method is applied for the three IRIP maps, as represented in

149    Figure 1. After reclassification, the generation map becomes an input indicator for the two other

150    maps of transfer and accumulation. The reclassification proceeds as follows: a pixel is favourable

151    (score = 1) if the generation susceptibility levels in its relative drained area have a mode (the most

152    present value of the distribution) higher than a user-defined susceptibility level (3 by default). The

153    use of the generation map as an input for the two others means that susceptibility to transfer or

154    accumulation is conditioned by a sufficiently high susceptibility for surface runoff generation. This

155    allows the incorporation of an upstream-downstream logic in the maps. For each map, the five

156    indicators have been chosen based on field knowledge (Dehotin et al., 2015a), literature review

157    (Dehotin and Breil, 2011b), and multiple combination tests.

158    For the surface runoff generation map, the five indicators are derived from factors influencing runoff

159    generation: soil properties, topography, and land use. Three indicators represent the impact of soil

160    properties and are based on soil erosion model parameters (Le Bissonnais et al., 2002; Le Gouee et

161    al., 2010; Nearing et al., 1989). The erodibility indicator in the generation map represents the

162    possibility of the generated surface water combining with soil particles to generate a mudslide

163    (Cerdà and Doerr, 2008). For agricultural plots, the erodibility indicator also represents the

164    susceptibility of soils to create slaking crusts that are favourable to surface runoff generation. The

165    topography indicator is an "or" combination of the slope and the topographic index, that is, the

166    topography indicator is favourable if the slope is steep, if the topographic index is high, or both.

167    Steep slopes are considered as favourable to surface runoff generation reflecting the reduced ability

168    of water to infiltrate into the soil. The topographic index (Beven and Kirkby, 1979), $ln(a/tanb)$, where

169    $a$ is the upstream drained area and $b$ is the local slope, reflects the capacity at one point to evacuate

170    water from upstream, that is, water storage-prone areas. Although the topographic index also uses

171    the slope, the topography indicator in the IRIP method combines two different effects: slope and

172    ability to store water. In order to be able to apply the method in every catchment without local

173    knowledge, relative thresholds ($t_1$, $t_2$) are used to distinguish topographic indicators (slopes,

174    topographic index) as favourable or not. For each indicator, the distinction is made thanks to

175    classification algorithms (MacQueen, 1967; Reuter et al., 2006). It permits dividing the study area

176    into two categories of slopes or topographic indices depending on the local and surrounding pixel

177    values. The land use indicator reflects the fact that urban and agricultural areas are considered as

178    favorable to surface runoff generation. For urban areas, the generation map is recalculated to force

179    soil permeability and thickness to be favourable in those areas, in the event that the areas have not

180    been classified as favourable from the indicators derived from the soil map.

181    The susceptibility maps of surface runoff transfer and accumulation reflect surface water natural-

182    flow dynamics. Both involve different mechanisms, acting often in the opposite direction, such as

183    slope and break of slope. This is why two maps are created. The choice of the corresponding

184    indicators is based on detailed analyses of past intense surface runoff events (Dehotin and Breil,

185    2011b) where slope, break of slope, catchment compactness, and artificial linear axes appeared as

186    main factors to produce intense phenomena. The computation of the break of slope proceeds as

187    follows: in each pixel, the mode of the slope value distribution in the upstream area drained by this

188    pixel is computed and compared to the local slope value of the pixel. If the upstream slope mode is

189    smaller (respectively higher) than the local slope, the pixel is indicated as convex (respectively

190    concave), and is assigned 1 for the transfer map (1 for the accumulation map). The transfer map uses

191    the Horton form factor (Horton, 1932), which is the ratio of area to length of the sub-watershed

192    defined by the drained area at the considered pixel. The artificial linear axes are taken into account in

193    the transfer map because of their role in surface runoff interception and displacement (Cerdà, 2007;

194    Pams-Capoccioni et al., 2015).

195    Finally, the input data of the IRIP method are: a DEM, a land use map, a soil map, and optionally the

196    artificial drainage network (Figure 1). The input data resolution can be adapted to the size of the

197    study area. For a relatively large study area, the analyst can proceed as follows: maps can be initially

198    produced for the whole study area with a coarse resolution DEM (i.e. cells larger than 10 meters) and

199    then areas susceptible to surface runoff can be focussed on with a higher resolution DEM (i.e. cells

200    smaller than 10 meters). These susceptibility maps reflect a certain description of the surface runoff

201    mechanisms in a watershed. Given the considered indicators, the IRIP map of surface runoff

202    generation highlights the areas more susceptible to generate water on the soil surface. The IRIP

203    transfer map highlights the areas where surface water can move and gain speed, and the IRIP map of

204    accumulation highlights the areas where there is a tendency for a reduction in surface water velocity

205    and water level increases. The method aims to be simple to implement, using open-access input data

206    and to be robust regardless of the data quality and uncertainty. This is the reason why more complex

207    methods such as weighting the indicators or classifying them into more than two categories were not

208    retained in the first version of the method. However, the method remains open for adaptation

209    regarding the user knowledge, but the default parametrization permits applying the method

210  whatever the study area. In this paper, the relevance of the IRIP maps is assessed based on this first

211  version of the method.

## 2.2. The Study Area

213  The Lézarde catchment (210 km²), located between the English Channel and the Seine river, is well-

214  known for being subject to flooding predominantly generated by surface runoff (Delahaye et al.,

215  2002; Douvinet et al., 2014; Le Gouee et al., 2010). The catchment morphology is composed of large

216  plateaux and narrow valleys (Figure 2). The permanent hydrographic network is very short but the

217  temporary network consists of an extremely dense talweg network. The area was formed during the

218  last glacial era during which the ice melt eroded the soil surface (Auzet et al., 1993). Soil

219  characteristics of the catchment are mostly silt and clay with flint stones. Locally, there are sandy

220  loams that increase soil erosion processes. The geology of the territory is composed of karst which

221  forms a complex active underground river network (Hauchard and Laignel, 2008). The climate of the

222  whole Seine-Maritime region is characterised by two main rainfall seasons: summer and autumn. In

223  summer, rainfall durations are shorter than in autumn but more intense, whereas in autumn the

224  rainfall patterns are less intense but last for long periods, leading to soil saturation (Douvinet, 2008).

225  These two rainfall patterns can both generate storm runoff floods but involve different mechanisms.

226  In terms of land use, a large part of the Lézarde catchment is made up of agricultural areas. A soil

227  crusting process takes place between planting cycles, influenced by an exposed and high silt rate in

228  the top soil, making the soil surface almost impervious (Robinson and Phillips, 2001). In addition,

229  roads and villages were built in exposed areas: many roads are located in talwegs and villages are

230  located at the downstream end of catchments or sub-catchments. Consequently, flooding in the

231  catchment tends to generate major damage.

232  In the Lézarde catchment, the IRIP maps were produced using a 25-meter DEM from the French

233  National Institute of Geograhy[2]. The land use map[3] is on the scale of 1/5000 in rural areas and 1/2000

234  in urban areas. The soil map is the pedologic map from the French National Institute for Agronomic

235  Research (INRA) at the scale of 1/1000000 (Dupuis, 1969). To calibrate the method in the Lézarde

236  catchment, some assumptions are made based on literature review, discussions with local

237  stakeholders and multiple tests on the IRIP maps. For the soil indicators, the distinction between

238  favorable or not is based on soil data analysis (Daroussin and King, 1997; Jamagne et al., 1995). The

239  slope threshold for the distinction between favorable or not was fixed at 4%, based on surface runoff

240  studies on the Lézarde catchment (Hauchard, 2002). For the land use indicator, the urbanized and

---

[2] http://professionnels.ign.fr/bdalti
[3] http://mos.hautenormandie.fr/Presentation

8

241    the agricultural areas are considered as favorable to surface runoff (Hauchard et al., 2002). For the

242    Horton form factor, the index is considered as favorable to surface runoff transfer for values larger

243    than 0.15 (fixed from tests with IRIP maps). Only roads and railways are used for the artificial linear

244    axes, as data on agricultural drainage are not available at this scale. The flow accumulation threshold

245    was chosen at 0.5 ha, a value small enough to detect surface runoff close to the catchment head.

246    These choices are explained further in the discussion and perspectives section.

### 247    2.3. The Comparison Data

248    The data sets used for the evaluation of the surface runoff susceptibility maps are presented here.

249    Four data sets are used: two regulatory zonings of surface runoff and erosion risks and two data sets

250    of surface runoff impacts on roads and railways networks. The two regulatory zonings are provided

251    by the agglomeration of Le Havre[4] and the local association of the Pointe de Caux Catchment[5]

252    (SMBV) respectively. They are part of the natural risk prevention plan (Departmental Directorate of

253    Seine-Maritime, 2013a; Departmental Directorate of Seine-Maritime, 2013b). These regulatory

254    zonings take into account both exposure of assets at risk and their probability of damage. The

255    database of surface runoff impacts on roads is provided by the SMBV and the database of surface

256    runoff impacts on railways is provided by the French National Railway Company (SNCF Réseau).

### 257    2.3.1. The Surface Runoff Regulatory Zoning

258    The surface runoff zoning was established in a qualitative manner. All the surface runoff axes, where

259    water can concentrate (i.e. the dry talwegs), were identified by field expertise and historical

260    information on past events (Hauchard, 2002). Then, to create the surface runoff zoning, a buffer area

261    around surface runoff axes was designed. The buffer size ranges from 5 to 80 meters and the value

262    was locally chosen thanks to field knowledge. Finally, hydrological modeling was used only in areas

263    with high exposure levels to obtain water levels and flow velocities, but the latter information is not

264    used in the evaluation procedure, where only the zoning map is used. This zoning map does not take

265    into account the presence of protection structures against floods.

266    For the comparison with IRIP, the surface runoff zoning is compared with the IRIP map of surface

267    runoff accumulation susceptibility. The zoning is created from the dry talweg axes, which are axes of

268    water concentration and where, locally, water velocity reduces and subsequently water depth

269    increases. This effect is included in the IRIP map of accumulation and is represented by the IRIP

270    indicators: flow accumulation, topographic index, and concave break of slopes. For the comparison

---

[4] http://www.codah.fr/article/lutte-contre-les-inondations
[5] http://www.smbv-pointedecaux.fr/web/decret_erosion2.html

271   tests, the permanent hydrographic network is also masked. Indeed, the accumulation map also

272   detects the rivers but the comparison rather focuses on hillslopes where surface runoff occurs.

### 2.3.2.   The Soil Erosion Regulatory Zoning

274   The soil erosion zoning was created using two soil erosion models: the RUSLE model from USDA

275   (Dabney et al., 2011) and the STREAM model from INRA (Cerdan et al., 2002). The models have been

276   adjusted using erosion traces from aerial photographs. The results of the two models have been

277   combined and validated by knowledge from local experts. The soil erosion hazard map was crossed

278   with a map of the territory vulnerabilities to obtain the soil erosion zoning map.

279   For the comparison with IRIP, the soil erosion zoning is compared with the IRIP map of surface runoff

280   transfer susceptibility. Indeed, the soil erosion is a process influenced by the occurrence of surface

281   runoff with a water level and a speed sufficient to transport materials. This effect is included in the

282   IRIP map of transfer and is represented by the IRIP indicators: compactness index and convex break

283   of slopes. For the comparison tests, the urban areas are masked because the regulatory zoning

284   focuses on rural areas.

### 2.3.3.   The Databases of Impacts on Transportation Networks

286   The database of flooded roads is made up of 31 road sections and was created after an intense

287   rainfall event by witness interviews and field expertise. On October 13, 2013, the Lézarde catchment

288   was subject to a significant rainfall event, generating intense surface runoff. The return period of the

289   event was estimated to be more than a hundred years by the Predict weather services (Gouvazé and

290   SMBV, 2013). The high-intensity rainfall affected mainly the three sub-catchments located in the

291   north of the Lézarde catchment, upstream of the Lézarde River (highlighted in yellow in Figure 3). Up

292   to 70 mm fell in 6 hours in this area and the three rain gages (1, 2, 3) recorded 160, 156 and 100 mm

293   respectively in 24 hours. Thus the comparison tests focus only on these 3 sub-catchments. The road

294   sections in the database were temporarily cut off by floodwater and impracticable or even swept

295   away by floodwater (photos at the bottom of Figure 3).

296   The database of impacts on the railway is made up of 41 incidents listed from 1995 to 2012. These 41

297   incidents are observed in 21 railway sections, the incidents occurring sometimes at the same

298   location. This database is not exhaustive and contains uncertainties on incident locations, particularly

299   in relation to the source of flooding and the length of railway that was affected. The recorded types

300   of incidents are embankment erosion, flooded platforms or mudslides. For the comparison tests,

301   these two databases are compared to the IRIP maps of transfer and accumulation susceptibility,

302   because we assume that accumulation as well as transfer of water can generate damage.

303   This section highlights that the four data sets differ greatly in form and content. The next section

304   describes the methodology used to compare these four data sets to the IRIP surface runoff

305   susceptibility maps.

306   **2.4. The Evaluation Method**

307   To evaluate the IRIP method, the surface runoff susceptibility maps are compared to a set of

308   comparison data. In this section, the comparison tests and the verification indicators are presented,

309   as well as the data formatting process that is required to compare different data types.

310   2.4.1.   Comparison Tests

311   To assess the correspondence between the IRIP maps and the comparison data, contingency tables

312   are created and associated verification indicators are computed. This method is inspired by the

313   standard verification methods for dichotomous (yes/no) forecasts (Hogan and Mason, 2012; Stanski

314   et al., 1989). Table 2 shows the theoretical contingency table created for each comparison test. The

315   "observed event" columns represent information from the comparison data. For example, in the case

316   of the zonings, "yes" means inside the zoning and "no" means outside. In the case of the impact

317   databases, "yes" means the impacted network section and "no" means the remaining parts of the

318   transportation network that were not impacted. The "IRIP" lines represent information from the IRIP

319   maps. For the tests, the IRIP maps are converted into dichotomous results, with "yes" being pixels

320   with a susceptibility level greater than or equal to 4 and "no" being pixels lower than 4. The

321   threshold of 4 is chosen regarding the low proportion of susceptibility level values of 4 and 5 over the

322   catchment. Pixel values of 4 and 5 represent 4% of the study area in average, whereas pixel values of

323   3 represents 30% of the study area. In the theoretical contingency table, for comparisons with the

324   regulatory zonings (respectively, comparisons with the impacts on the transportation network), true

325   positives are IRIP pixels with high susceptibility levels located inside the zonings (resp. inside the

326   impacted network sections). True negatives are IRIP pixels with low susceptibility levels located

327   outside the zonings (resp. inside the not impacted network sections). False positives are IRIP pixels

328   with high susceptibility levels located outside the zonings (resp. inside the not impacted network

329   sections). Finally, false negatives are IRIP pixels with low susceptibility levels located inside the

330   zonings (resp. inside the impacted network sections). From the contingency tables, five verification

331   indicators are computed: accuracy, bias, success ratio (SR), probability of detection (POD), and false

332   alarm ratio (FAR). POD and FAR are computed only when comparing with the impacts on the

333   transportation network, in order to assess the ability of the IRIP method to detect areas susceptible

334   to be impacted. The indicators are presented in Table 3 along with the formulas and the result

335   interpretations.

336      2.4.2.    Data Formatting

337      Concerning comparison tests with the regulatory zonings, the surface runoff regulatory zoning is

338      compared with the IRIP map of accumulation susceptibility. The soil erosion zoning is compared with

339      the IRIP map of transfer susceptibility. For each comparison, the contingency table is computed by

340      using two different thresholds of IRIP susceptibility level: for pixel values greater than or equal to 4

341      and for pixel values of 5 only. Moreover, for each comparison, the contingency table is computed by

342      using three different sizes of buffer area around the zonings: 0, 25, and 50 meters. Buffer areas are

343      used in order to compensate for uncertainties in data comparison. Uncertainties can come from the

344      fact that different data formats are compared (raster for the IRIP map and polygons for the zonings).

345      This can lead to uncertainty when overlapping the data. Uncertainties can also come from the input

346      data used for the creation of the IRIP maps and the zonings (i.e. DEM resolution). Buffer area sizes of

347      0, 25, and 50 meters correspond to a shift of zero, one or two pixels of the IRIP maps.

348      Concerning the impact databases, comparison tests are performed separately for roads and railways,

349      and for each test, the impact locations are compared with the IRIP maps of transfer and

350      accumulation simultaneously. The comparisons are performed using the transportation network as

351      the reference study area, and not the whole catchment. In order to perform the comparison, the

352      linear transportation networks are transformed to polygons, using a buffer. Two buffer area sizes of

353      25 and 50 meters on both sides of the transportation network were considered. Concerning the IRIP

354      maps, an area is considered susceptible to surface runoff if there is a spatial persistence of pixels

355      with high susceptibility levels, and not if there is only one isolated pixel with a high value. The pixel

356      spatial persistence on the IRIP maps of transfer and accumulation is taken into account as follows: a

357      buffer area of 25 meters is drawn around all pixels of values 4 and 5 and, if an isolated pixel with its

358      buffer area is not intercepted by another buffer, the pixel is removed (Figure 4a). Finally, four

359      contingency tables are computed for roads and railways with two different buffer area sizes around

360      the transportation network, focusing on the overlapping surface between the IRIP maps and the

361      impacted road sections, as presented in Figure 4b.

362

363      **3.   Results**

364      **3.1. Application of the IRIP method in the Lézarde catchment**

365      The susceptibility map of surface runoff generation (Figure 5) shows that the catchment presents a

366      high susceptibility to generate surface runoff. About 88% of the study area has pixels with a score

367      above 3, on a scale ranging from 0 to 5. The pixels with a highest score are located in the urban areas

368    of Le Havre and Montivilliers. We can also see high susceptibility levels in the western part of the

369    catchment and in the valley sides. Although the valley sides are occupied by forest, they present a

370    high susceptibility to generate surface runoff because of soil properties and steep slopes. Despite the

371    flat topography of the plateaux upstream of the catchment, they present a high susceptibility to

372    surface runoff generation with values of 3 and 4 locally because of the soil properties and the

373    agricultural land use. Occupying approximately two thirds of the catchment, these plateaux are

374    responsible for the largest part of the generated surface water.

375    The susceptibility map of surface runoff transfer (Figure 6) mainly shows high levels in the valley

376    sides, where slopes are steep and break of slopes are convex. This map shows low susceptibility

377    values of transfer in the plateaux and in the valley bottom. The high susceptibility areas actually

378    highlight the sides of the main talwegs and a great deal of small talwegs even very close to the head

379    of the catchment.

380    The susceptibility map of surface runoff accumulation (Figure 7) shows that plateaux are prone to

381    accumulate surface runoff with values equal or greater than 3 on a large part of the catchment.

382    These susceptibility levels are due to low slopes, concave break of slopes, and a high topographic

383    index in the upstream portions of the catchment. Permanent rivers are identified with the level 5,

384    and an extremely dense talweg network can be distinguished with the susceptibility levels 4 and 5. In

385    upstream talwegs, susceptibility levels 4 and 5 are still visible but seem to be more spread out. The

386    map highlights that the valley sides are not favorable to surface runoff accumulation in contrast to

387    the map of transfer.

388        **3.2. Evaluation of the IRIP maps**

389    In this section, the IRIP maps are first compared to the regulatory zonings, in order to assess the

390    ability of the map of accumulation to identify areas prone to concentrated surface runoff (Figure 8)

391    and to assess the ability of the map of transfer to identify areas prone to soil erosion (Figure 9). Then,

392    the IRIP maps are compared to the databases of impacts on the transportation network to assess the

393    ability of the IRIP method to identify road and railway sections susceptible to be impacted by surface

394    runoff (Figure 10).

395    The superimpositions of the IRIP maps and the two regulatory zonings (Figures 8 and 9) show a good

396    visual correlation and a relevance of the spatial distribution of the IRIP susceptibility levels. Table 4

397    presents the results of the comparison between the two regulatory zonings and the IRIP maps. Six

398    comparison tests are performed for the surface runoff zoning and six for the soil erosion zoning: with

399    the three buffer area sizes and considering pixels of value 4 and 5, and 5 only. Three indicators are

400    computed for each test: accuracy, bias, and success ratio. Results show that for that comparison with

401    the surface runoff zoning, the accuracy ranges from 0.68 to 0.86 and, for the comparison with the

402    soil erosion zoning, accuracy ranges from 0.36 to 0.69. Biases for all the tests are lower than 1 and

403    range from 0 to 0.41. The success ratio represents the number of high susceptibility level pixels that

404    are located inside the zoning, regarding the whole study area. It ranges from 0.41 to 0.92. The best

405    success ratio for the accumulation map is 0.92 and is obtained when using a 50-meter buffer around

406    the surface runoff zoning and when considering only pixels with a value of 5. The best success ratio

407    for the transfer map is also 0.92 and obtained with the same conditions. Moreover, a success ratio of

408    0.91 is obtained when considering pixels of value 4 and 5, using a 50-meter buffer. Concerning the

409    comparison with the impacts on the transportation network, Table 5 shows the results of the five

410    verification indicators for the four tests: comparison with the database of impact on roads and with

411    the database of impacts on railways, using two different buffer area sizes for both of 25 and 50

412    meters around the transportation network. For the analysis of impacts on roads, comparison tests

413    show accuracy of about 0.6 and 0.3 for impacts on railways. Biases are greater than 1 and range

414    approximately from 3 to 9. Success ratios are lower than 0.25 for both transportation networks.

415    Probabilities of detection range from 0.7 to 0.9, and figures are similar for the false alarm ratios. The

416    best probability of detection for the impacted road sections is 0.73 using a 25-meter buffer around

417    roads, and the best one for the impacted railway sections is 0.9 using a 50-meter buffer around

418    railways.

419    These results are discussed in the next section in the light of the assumptions made for the

420    comparison tests and in the light of the high false alarm ratios for the comparison tests with the

421    impact databases. Moreover, suggestions are presented to go further in the evaluation method and

422    in the development of the IRIP method.

423

424

425

426    **4.    Discussion and Perspectives**

427    **4.1. Result Discussion**

428    **4.1.1. Comparisons with the Regulatory Zonings**

429    The success ratio is the number of pixels with high susceptibility levels located inside the zonings

430    regarding the total number of pixels with high susceptibility levels in the catchment. So, without

431    using a buffer, obtaining success ratios of 0.72 and 0.64 is already promising. Using a buffer area of

432    50 meters around the zonings makes it possible to obtain success ratios above 0.9. This shows that a

433    large number of high susceptibility IRIP pixels are located very close to the regulatory zonings and

434    that uncertainties in the high susceptibility level locations could be interpreted as between 0 and 2

435    pixels. These success ratios are extremely promising considering that the two maps are created using

436    very different techniques and that they do not focus exactly on the same areas. The soil erosion

437    zoning focuses on agricultural areas, and the surface runoff zoning focuses on talweg axes, whereas

438    the IRIP method takes into account the whole catchment. Different results are obtained when

439    considering pixel values of 5 and pixel values of 4 and 5 together. The choice of the susceptibility

440    level depends on the information sought. Few pixels with a value of 5 are present in the catchment.

441    They underestimate the global sensitivity of the catchment (bias close to zero), but they are more

442    likely to indicate the localization of the areas that are highly susceptible to surface runoff. Concerning

443    the IRIP map of accumulation, Figure 8 shows that the pixels are located precisely inside the zoning in

444    the downstream part of the catchment but, in the catchment headwaters, pixels with a value of 4 are

445    spread and are located outside the zoning. This spatial persistence of pixel values of 4 could indicate

446    the beginning of a talweg that is not well defined in the landscape. Further comparison tests and field

447    analysis must be undertaken to confirm this hypothesis.

448    Moreover, Figure 9 shows that a considerable section of areas contained in the erosion zoning is not

449    correlated with the IRIP map of transfer, but seems to fit with the IRIP map of accumulation (Figure

450    11). Indeed, these areas present lower slopes, concave break of slopes, high topographic indices, and

451    high flow accumulations. The soil erosion zoning gives a map of soils prone to erosion but, depending

452    on the areas, erosion mechanisms and impacts can be different. The transfer map could emphasize

453    incision susceptibility and the accumulation map could localize the deposit areas. Field analysis must

454    be undertaken to better assess the ability of the IRIP maps to identify different erosion processes,

455    but knowing the spatial distribution of the dominant processes could permit adapting the erosion

456    prevention techniques in terms of the mechanisms involved.

457    Finally, the comparison with the two regulatory zonings shows that the maps produced with the IRIP

458    method seems to be relevant in identifying areas susceptible to surface runoff. Moreover,

459    susceptibility levels of 5 seem to indicate with a certainty of 90% an area susceptible to concentrative

460    surface runoff (for the IRIP map of accumulation) and an area susceptible to soil erosion (for the IRIP

461    map of transfer) with a spatial accuracy from 0 to 2 pixels.

462

463

464        **4.1.2. Comparisons with Impacts on the Transportation Network**

465

466        The probability of detection is the ratio of good detection over the total observed impacts. Obtaining

467        probabilities of detection of 0.7 for road impacts and 0.8 for railway impacts is promising. The IRIP

468        method seems to be relevant in identifying areas susceptible to surface runoff. However, success

469        ratios are low due to a significant number of false alarms (i.e. false positives). The highly significant

470        false alarm ratios and the overestimation are discussed.

471        First, these results come from the fact that the IRIP method gives susceptibility maps regarding soil

472        surface predisposition, but the occurrence of a surface runoff-related impact depends on the rainfall

473        spatial variability. For the rainfall event of October 13, 2013, it is assumed that rainfall was spatially

474        homogeneous in the three sub-catchments, but this hypothesis is no more realistic for the railway

475        network because the study area is wider and the database ranges in time from 1995 to 2012, when

476        rainfall events are not likely to have been homogeneous. This can explain why higher false alarm

477        ratios are obtained for the analysis of railway impacts. Moreover, working with proxy data involves

478        uncertainties. For example, the databases may suffer from a lack of exhaustiveness in the number of

479        reported impacts. In that case, impacts only are reported, whereas some network sections could

480        have been affected by floodwater without being damaged and without network managers being

481        informed. In addition to this, high false alarm ratios can come from the fact that the IRIP maps, which

482        represent a susceptibility of surface runoff occurrence, are compared to an impact which is an

483        effective risk. It is essential to take the structural vulnerability of roads and railways into account for

484        a better assessment of the IRIP maps' ability to identify impacted sections.

485        Concerning the impacted roads analysis, more than 40 hydraulic structures are present over the

486        three sub-catchments where intense rainfall occurred on October 13, 2013. They probably played an

487        important role in the protection of the road network. Figure 10 shows the road network of the three

488        sub-catchments along with the hydraulic structure locations. Post-event investigation allowed

489        reporting whether or not the hydraulic structures have played their protective role. Green points

490        indicate that the structure did not overflow; orange points indicate that it overflowed. This

491        information can already explain why some road sections that appear susceptible to surface runoff

492        with the IRIP method have not been reported as impacted. For example, in Figure 12, the A photo

493        (corresponding to the A area on Figure 10) was taken just after the event and shows that the dam

494        closing a reservoir is at one meter below the overflow. Thus, it could have protected this road section

495        against floodwater. Further discussions with the river basin managers helped to explain some other

496        false alarms. Figure 12 shows photos of three road sections (B, C, and E areas can be seen in Figure

497     10) that are considered as false alarms, despite the absence or dysfunction of protective structures.

498     These photos show the configuration of roads within their environment, and give some clues about

499     the vulnerability level of the sections regarding surface runoff. Photo B shows a large drainage ditch

500     along the road. Photo C shows the road slightly elevated and the low point located in the grassland.

501     These observations have been confirmed by the river basin managers. They also attested that the

502     road section in the A area is regularly flooded by surface runoff during intense rainfall events and

503     that the low point in the D area is not located on the road but in the nearby field. The three impacts

504     in the E area present the same configuration, that is, they transversally cut a dry talweg without any

505     crossing structure. Photo E shows one of these intersections which still have the marks of an intense

506     rainfall event, with standing water and soil deposits gathered in a mound. This configuration can

507     explain why IRIP detects smaller susceptible areas than the reported section for these three impacts.

508     The road may act as a barrier to the water flow path. Water can spread on both sides along the road

509     and consequently flood a large section of the road. Using a DEM with a better resolution could help

510     in identifying the local configuration. Finally, according to the river basin managers, the F area has

511     been less exposed to the rainfall event, which can explain why it has not been reported as impacted.


512     For railways, the infrastructure configuration is more complex. Indeed, railway structures are highly

513     constrained to keep a steady inclination and do not follow the natural topography. Railways are

514     often built on embankments or in cuttings of varying height or depth. These configurations make

515     railways vulnerable to surface runoff. To protect the railway infrastructure, multiple drainage devices

516     or crossing structures are present all along the tracks to intercept flow paths and redirect them

517     downstream. Therefore, to better identify railway sections susceptible to being impacted by surface

518     runoff, the vulnerability must be characterized. The configuration of the infrastructure itself must be

519     defined but the level of maintenance of the hydraulic structures must also be taken into account.


520

521     ### 4.2. Further Analysis with the Evaluation Method

522     In the evaluation method, we need to compare data that do not have the same shape, do not give

523     the same information, and that have been acquired using different techniques. Suitable indicators

524     must be used to show the correspondence between data and to quantify it. For example, the success

525     ratio gives information on whether or not the pixels with a high susceptibility level are located inside

526     the zoning, but do not inform on the spatial distribution of the pixels regarding the zoning. For

527     further evaluation, more complex indices could be used in order to improve the correlation analysis,

528     for example by focusing on the shape of strong pixel areas or by analyzing pixel surroundings and

529     mitigating isolated pixel effects (Hagen-Zanker, 2009; Hargrove et al., 2006).

530    For the comparison tests, assumptions have been made and preliminary treatments have been

531    carried out on the comparison data and on the IRIP map. Choices have been made for this study and

532    must be discussed. First, pixels with a value of 4 and 5 are considered as high susceptibility levels.

533    The significance of the susceptibility level 5 has been shown, but the significance of level 4 must be

534    assessed. The significance of level 3 must also be assessed. Is it really not significant? Do levels 0, 1,

535    and 2 indicate no surface runoff sensitivity? Moreover, for the comparison tests, buffer areas have

536    been used. In order to avoid arbitrary choice on the buffer area size, the tests have been performed

537    using 2 different sizes of 25 and 50 meters but more sizes could be tested, particularly negative

538    buffer areas (reducing the zoning). For the comparison with the impacts on the transportation

539    network, the hypothesis on the spatial persistence of high susceptibility levels indicating areas

540    susceptible to be impacted must be assessed, along with the significance of isolated pixels. Do they

541    bring valuable information or noise due to eventual input data inaccuracy?

542    Moreover, this study focuses on the transfer and the accumulation maps. For further evaluation, it

543    would be interesting to focus on the susceptibility map to surface runoff generation and evaluate its

544    ability to detect areas susceptible to generate significant quantities of surface water. For example,

545    for the impact databases, it would be interesting to use the map of generation in a second phase, to

546    help in distinguishing the sections most susceptible to be impacted among the ones detected by the

547    maps of transfer and accumulation. Sections with a large area upstream with high susceptibility

548    levels of surface runoff generation could be susceptible to be impacted with relatively major

549    quantities of water or more often, or to be impacted first during a rainfall event. This hypothesis

550    must be evaluated.

551    For further evaluation of the ability of the IRIP method to detect sections of the transportation

552    network susceptible to be impacted by surface runoff, the structural vulnerability of the network

553    must be characterised. A vulnerability indicator with different levels could be defined on the whole

554    network, in order to combine hazards and vulnerability better and to correlate the location of

555    impacts more effectively. Concerning the impacts, for such a comparison, further research must be

556    undertaken to improve the completeness of the databases. In addition to these tests, particular

557    events must be analyzed in greater detail in order to consider the influence of rainfall characteristics

558    and better assess the surface runoff flow dynamic. To confirm the results obtained in this study,

559    further comparison tests must be performed with different comparison data and for different study

560    areas with other hydrological contexts.

561

562    **4.3. Further Analysis with the IRIP Method Development**

563    Several options for further developing and improving the IRIP method can be proposed. Concerning

564    the map of susceptibility to surface runoff generation, the valley sides appear as favorable to surface

565    runoff whereas in reality the plateaux are the most important sources of surface runoff generation

566    due to their relative importance in terms of proportion of the catchment size and to the fact that

567    they are cultivated. They can generate substantial quantities of surface runoff which can be

568    transferred to the valley throughout the extremely dense dry talweg network. It would be interesting

569    to be able to integrate these geomorphology features in the IRIP method. For example, a

570    computation of geomorphologic indexes could permit calibrating the method in terms of the

571    plateau/valley distribution. The default configuration of the method is that steep slopes are

572    favorable to surface runoff generation, which is relevant for mountainous areas, for example, but

573    this choice could be inversed when working on large flat areas with large agricultural fields.

574    Furthermore, the susceptibility map of surface runoff generation could be improved with better data

575    accuracy. Especially the soil map, which is used for three of the five indicators, has a resolution of

576    1/1000000 and gives only six different soil units in the Lézarde catchment. Moreover, it has been

577    shown that the geology has an influence on surface runoff generation and transfer (Onda et al.,

578    2001); it would be interesting to use this parameter in the IRIP method.

579    The map of susceptibility to surface runoff transfer takes the artificial linear axes as an input indicator

580    because they can modify surface runoff directions, but if the data are available it would be

581    interesting to add the urban and agricultural drainage network in this indicator. For the creation of

582    this map, we currently use the Horton form factor to reflect the compactness effect of the sub-

583    catchment drained by each pixel (0.15 for our study). This index is not particularly satisfying because

584    of its instability when computed on small drained areas. More adapted compactness indexes must be

585    tested (Gravelius, 1914; Schumm, 1956), although their implementation can be complex with GIS

586    techniques (Bardossy and Schmidt, 2002; Bendjoudi and Hubert, 2002). It would be better to use an

587    index that is more adapted to a distributed computation.

588    In addition to these suggestions, the IRIP method could also be improved by making additional tests.

589    For example, stability tests on the indicator thresholds could be performed to evaluate the threshold

590    computation method. Changes in the input data resolution (DEM, land use map, and soil map) could

591    be studied to evaluate how it affects the resulting maps. It would also be interesting, from a risk

592    point of view, to cross the IRIP maps with meteorological data or land use change monitoring to

593    provide real-time probability maps.

594

595    **5.  Conclusions**

596   This paper presents the IRIP method for surface runoff susceptibility mapping and its evaluation by
597   comparison with different datasets. The method makes it possible to produce three maps
598   representing different surface runoff mechanisms: generation, transfer, and accumulation. The
599   maps' evaluation shows a significant correspondence between the IRIP map of accumulation and the
600   surface runoff regulatory zoning and between the IRIP map of transfer and the soil erosion zoning.
601   The comparison with data of impacts on the transportation network show promising probabilities of
602   detection which confirm the relevance of the susceptibility maps. For an operational need of network
603   monitoring, the structural vulnerability must be characterized to better discriminate the false alarms.

604   The IRIP method has shown promising results during the comparison tests, but can it be used as a
605   tool for risk management? The IRIP method aims to be simple to implement and requires few input
606   data that are widely available. Neither specific study area size nor calibration is required for a first
607   use. In this sense, the IRIP method can be a useful tool to get a first understanding of the surface
608   runoff mechanisms involved in a catchment and of their spatial distribution. Nonetheless, to go
609   further in the map analysis, field expertise is required. The use of the IRIP maps regarding the usual
610   hazard assessment methods can be complex because of the three types of maps and the
611   susceptibility scale. In the other hand, working with three susceptibility maps of generation, transfer,
612   and accumulation gives the opportunity to adapt risk mitigation techniques depending on the areas.
613   In the areas prone to surface runoff generation, one can avoid soil imperviousness or facilitate
614   infiltration with reservoir basins. In the surface runoff transfer areas, one can avoid bare soils and
615   obstacles susceptible to be swept away. For accumulation areas, one can try to reduce stake
616   vulnerabilities. Finally, this study highlights that a multidisciplinary approach is essential to assess
617   surface runoff hazards. Likewise, a systemic view of the whole catchment is required, along with
618   interactive work with the catchment stakeholders, to improve surface runoff risk management and
619   to sustainably develop territories.

620

621

622

623   **Acknowledgments**

632    **References**

633    Abudi, I., Carmi, G., Berliner, P., 2012. Rainfall simulator for field runoff studies. J. Hydrol. 454, 76–81.

634    Akgun, A., Türk, N., 2010. Landslide susceptibility mapping for Ayvalik (Western Turkey) and its
635            vicinity by multicriteria decision analysis. Environ. Earth Sci. 61, 595–611.

636    Arnaud, P., Dehotin, J., 2011. Surface runoff hazard estimation methods - Comparison of the SHYREG
637            and the IRIP methods. IRSTEA Aix-en-Provence et IRSTEA Lyon.

638    Auzet, A.V., Boiffin, J., Papy, F., Ludwig, B., Maucorps, J., 1993. Rill erosion as a function of the
639            characteristics of cultivated catchments in the north of France. Catena 20, 41–62.
640            doi:10.1016/0341-8162(93)90028-N

641    Bardossy, A., Schmidt, F., 2002. GIS approach to scale issues of perimeter-based shape indices for
642            drainage basins. Hydrol. Sci. J.-J. Sci. Hydrol. 47, 931–942. doi:10.1080/02626660209493001

643    Bendjoudi, H., Hubert, P., 2002. The Gravelius compactness coefficient: critical analysis of a shape
644            index for drainage basins. Hydrol. Sci. J. 47, 921–930. doi:10.1080/02626660209493000

645    Beven, K.J., Kirkby, M.J., 1979. A physically based, variable contributing area model of basin
646            hydrology / Un modèle à base physique de zone d'appel variable de l'hydrologie du bassin
647            versant. Hydrol. Sci. J. 24, 43–69. doi:10.1080/02626667909491834

648    Buckle, P., Mars, G., Smale, S., 2000. New approaches to assessing vulnerability and resilience. Aust.
649            J. Emerg. Manag. 15, 8.

650    Carpenter, T.M., Sperfslage, J.A., Georgakakos, K.P., Sweeney, T., Fread, D.L., 1999. National
651            threshold runoff estimation utilizing GIS in support of operational flash flood warning
652            systems. J. Hydrol. 224, 21–44. doi:10.1016/S0022-1694(99)00115-8

653    Cerdà, A., 2007. Soil water erosion on road embankments in eastern Spain. Sci. Total Environ. 378,
654            151–155. doi:10.1016/j.scitotenv.2007.01.041

655    Cerdà, A., Doerr, S.H., 2008. The effect of ash and needle cover on surface runoff and erosion in the
656            immediate post-fire period. Catena 74, 256–263. doi:10.1016/j.catena.2008.03.010

657    Cerdan, O., Souchere, V., Lecomte, V., Couturier, A., Le Bissonnais, Y., 2002. Incorporating soil surface
658            crusting processes in an expert-based runoff model: Sealing and Transfer by Runoff and
659            Erosion related to Agricultural Management. Catena 46, 189–205. doi:10.1016/S0341-
660            8162(01)00166-7

661    Chazelle, B., Lambert, L., Capoccioni, C.P., 2014. Railway vulnerability in case of extremes floods.
662            Knowledge and risk management. Houille Blanche 48–54. doi:10.1051/lhb/2014016

663    Christensen, F.M., Andersen, O., Duijm, N.J., Harremoës, P., 2003. Risk terminology—a platform for
664            common understanding and better communication. J. Hazard. Mater. 103, 181–203.
665            doi:10.1016/S0304-3894(03)00039-6

666    Cros-Cayot, S., 1996. Distribution spatiale des transferts de surface à l'échelle du versant. Contexte
667            armoricain. Ecole Nationale Supérieure Agronomique de Rennes.

668    Dabney, S.M., Yoder, D.C., Vieira, D.A.N., Bingner, R.L., 2011. Enhancing RUSLE to include runoff-
669            driven phenomena. Hydrol. Process. 25, 1373–1390. doi:10.1002/hyp.7897

670    Daroussin, J., King, D., 1997. A pedotransfer rules database to interpret the soil geographical
671            database of Europe for environmental purposes. Presented at the the workshop on the use
672            of pedotransfer in soil hydrology research in Europe, Orléans, FRA, pp. 25–40.

673    Defrance, D., 2014. Adaptation and evaluation of a flash flood warning system in ungauged
674            mountainous catchments (Earth Sciences). Université Pierre et Marie Curie - Paris VI.

675    Dehotin, J., Breil, P., 2011a. Technical report of the IRIP project: mapping the flooding by runoff
676            (Technical report). IRSTEA Hydrology-Hydraulic Research Unit.

677    Dehotin, J., Breil, P., 2011b. IRIP project: Research bibliographic report on surface runoff mapping
678            (Literature review). IRSTEA Hydrology-Hydraulic Research Unit.

679    Dehotin, J., Breil, P., Braud, I., de Lavenne, A., Lagouy, M., Sarrazin, B., 2015a. Detecting surface
680            runoff location in a small catchment using distributed and simple observation method. J.
681            Hydrol. 525, 113–129. doi:10.1016/j.jhydrol.2015.02.051

682    Dehotin, J., Chazelle, B., Laverne, G., Hasnaoui, A., Lambert, L., Breil, P., Braud, I., 2015b. Applying
683        runoff mapping method IRIP for flooding risk analysis on railway infrastructure. Houille
684        Blanche 56–64. doi:10.1051/lhb/20150069
685    Delahaye, D., Guermond, Y., Langlois, P., 2002. Spatial interaction in the run-off process. Cybergeo
686        Eur. J. Geogr. doi:10.4000/cybergeo.3795
687    Departmental Directorate of Seine-Maritime, 2013a. Flood Risk Prevention Plan - Presentation
688        report.
689    Departmental Directorate of Seine-Maritime, 2013b. Flood Risk Prevention Plan of the Lezarde
690        Catchment - Application rules.
691    DeRoo, A.P.J., Wesseling, C.G., Ritsema, C.J., 1996. LISEM: A single-event physically based
692        hydrological and soil erosion model for drainage basins .1. Theory, input and output. Hydrol.
693        Process. 10, 1107–1117. doi:10.1002/(SICI)1099-1085(199608)10:8<1107::AID-
694        HYP415>3.0.CO;2-4
695    Douvinet, J., 2008. Les bassins versants sensibles aux « crues rapides » dans le Bassin Parisien –
696        Analyse de la structure et de la dynamique de systèmes spatiaux complexes. Université de
697        Caen/Basse-Normandie.
698    Douvinet, J., Delahaye, D., Langlois, P., 2008. Modélisation de la dynamique potentielle d'un bassin
699        versant et mesure de son efficacité structurelle. Cybergeo Eur. J. Geogr.
700        doi:10.4000/cybergeo.16103
701    Douvinet, J., Wiel, M.J.V.D., Delahaye, D., Cossart, E., 2014. A flash flood hazard assessment in dry
702        valleys (northern France) by cellular automata modelling. Nat. Hazards 75, 2905–2929.
703        doi:10.1007/s11069-014-1470-3
704    Dupuis, J., 1969. La carte pédologique de la France au millionième. Rev. Géographie Alp. 219–219.
705    Faulkner, H., Boardman, J., Ruiz, J.-L., 2010. A simple validated GIS expert system to map relative soil
706        vulnerability and patterns of erosion during the muddy floods of 2000–2001 on the South
707        Downs, Sussex, UK. Land Degrad. Dev. 21, 310–321. doi:10.1002/ldr.1005
708    Galevski, M., 1955. La corrélation entre les pluies torrentielles et l'intensité de l'érosion (Field
709        observation report).
710    Gouvazé, J., SMBV, 2013. Floods of 13 & 14 October 2013: feedback on this unusual weather event.
711    Gravelius, H., 1914. Grundriss der gesamten Gewässerkunde: in vier Bänden. 1. Flusskunde,
712        Compendium of Hydrology, vol. 1: Rivers. Göschen, Berlin, Germany.
713    Guillobez, S., Lompo, F., De Noni, G., 2000. Le suivi de l'érosion pluviale et hydrique au Burkina Faso.
714        Utilisation d'un modèle cartographique. Sci. Chang. Planétaires Sécher. 11, 163–9.
715    Hagen-Zanker, A., 2009. An improved Fuzzy Kappa statistic that accounts for spatial autocorrelation.
716        Int. J. Geogr. Inf. Sci. 23, 61–73. doi:10.1080/13658810802570317
717    Hargrove, W.W., Hoffman, F.M., Hessburg, P.F., 2006. Mapcurves: a quantitative method for
718        comparing categorical maps. J. Geogr. Syst. 8, 187–208. doi:10.1007/s10109-006-0025-x
719    Hauchard, E., 2002. Risk Prevention Plan for floods and surface runoff. Methodol. Defin. Surf. Runoff
720        Hazard Hydrogeomorphological Approach Dep. Equip. Dir. 76.
721    Hauchard, E., Delahaye, D., Freiré-Diaz, S., 2002. Fractal organization of the soil occupation:
722        consequences on the runoff and gully erosion in arable cropping areas. Géomorphologie
723        Relief Process. Environ. 8, 181–196.
724    Hauchard, E., Laignel, B., 2008. Morphotectonic evolution of the north-western margin of the Paris
725        Basin. Z. Für Geomorphol. 52, 463–488. doi:10.1127/0372-8854/2008/0052-0463
726    Hewlett, J.D., 1982. Principles of forest hydrology. University of Georgia Press.
727    Hewlett, J.D., Hibbert, A.R., 1967. Factors affecting the response of small watersheds to precipitation
728        in humid areas. For. Hydrol. 275–290.
729    Hogan, R.J., Mason, I.B., 2012. Deterministic forecasts of binary events. Forecast Verification Pract.
730        Guide Atmospheric Sci. Second Ed. 31–59. doi:10.1002/9781119960003.ch3
731    Holzmann, H., Sereinig, N., 1997. In situ measurements of hillslope runoff components with different
732        types of forest vegetation. IAHS PRESS WALLINGFORD ENGL 317–324.

733    Horton, R.E., 1933. The role of infiltration in the hydrologic cycle. Trans. Am. Geophys. Union 14,
734          446–460. doi:10.1029/TR014i001p00446
735    Horton, R.E., 1932. Drainage-basin characteristics. Trans. Am. Geophys. Union 13, 350.
736          doi:10.1029/TR013i001p00350
737    Hudson, N., 1993. Field measurement of soil erosion and runoff. Food & Agriculture Org.
738    IPCC, 2003. IPCC Third Assessment Report - Climate Change 2001: 2.3.2.1 Palaeoclimate proxy
739          indicators.
740    Jamagne, M., Hardy, R., King, D., Bornand, M., 1995. La base de données géographique des sols de
741          France. Etude Gest. Sols 2, 153–172.
742    Javelle, P., Demargne, J., Defrance, D., Pansu, J., Arnaud, P., 2014. Evaluating flash-flood warnings at
743          ungauged locations using post-event surveys: a case study with the AIGA warning system.
744          Hydrol. Sci. J. 59, 1390–1402. doi:10.1080/02626667.2014.923970
745    Laflen, J., Lane, L., Foster, G., 1991. Wepp - a New Generation of Erosion Prediction Technology. J.
746          Soil Water Conserv. 46, 34–38.
747    Langlois, P., Delahaye, D., 2002. RuiCells, automate cellulaire pour la simulation du ruissellement de
748          surface. Rev. Int. Géomat. 12, 461–487.
749    Laverne, G., 2013. Application and validation of a runoff areas mapping tool in the railway context:
750          identification of sites subject to flooding by runoff (Master thesis). IRSTEA Hydrology-
751          Hydraulic Research Unit.
752    Le Bissonnais, Y., Montier, C., Jamagne, M., Daroussin, J., King, D., 2002. Mapping erosion risk for
753          cultivated soil in France. Catena 46, 207–220. doi:10.1016/S0341-8162(01)00167-9
754    Le Gouee, P., Delahaye, D., Bermond, M., Marie, M., Douvinet, J., Viel, V., 2010. SCALES: a large-scale
755          assessment model of soil erosion hazard in Basse-Normandie (northern-western France).
756          Earth Surf. Process. Landf. 35, 887–901. doi:10.1002/esp.1942
757    Legros, J., 2014. Study of datas given by a method of flooding harzard by surface runoff in flow
758          discharge modelling linked with this kind of flooding (Master thesis). IRSTEA Hydrology-
759          Hydraulic Research Unit.
760    MacQueen, J., 1967. Some methods for classification and analysis of multivariate observations.
761          Presented at the the fifth Berkeley symposium on mathematical statistics and probability,
762          Oakland, CA, USA., pp. 281–297.
763    Moriasi, D.N., Arnold, J.G., Van Liew, M.W., Bingner, R.L., Harmel, R.D., Veith, T.L., 2007. Model
764          evaluation guidelines for systematic quantification of accuracy in watershed simulations.
765          Trans. Asabe 50, 885–900. doi:10.13031/2013.23153
766    Naulin, J.-P., Payrastre, O., Gaume, E., 2013. Spatially distributed flood forecasting in flash flood
767          prone areas: Application to road network supervision in Southern France. J. Hydrol. 486, 88–
768          99. doi:10.1016/j.jhydrol.2013.01.044
769    Nearing, M.A., Foster, G.R., Lane, L.J., Finkner, S.C., 1989. Erosion Prediction Project Technology.
770    Onda, Y., Komatsu, Y., Tsujimura, M., Fujihara, J., 2001. The role of subsurface runoff through
771          bedrock on storm flow generation. Hydrol. Process. 15, 1693–1706. doi:10.1002/hyp.234
772    Ortega, K.L., Smith, T.M., Manross, K.L., Kolodziej, A.G., Scharfenberg, K.A., Witt, A., Gourley, J.J.,
773          2009. The severe hazards analysis and verification experiment. Bull. Am. Meteorol. Soc. 90,
774          1519–1530.
775    Pams-Capoccioni, C., Nivon, D., Amblard, J., De cesare, G., Ghilardi, T., 2015. Risk analysis for railway
776          traffic of overflowing of the drainage system on High Speed Lines. Houille Blanche 39–45.
777          doi:10.1051/lhb/20150044
778    Piney, S., 2009. Etude bibliographique de trois méthodologies appliquées au risque érosion: synthèse
779          et perspective en vue d'une cartographie départementale du risque de ruissellement.
780    Pons, F., Delgado, J.-L., Guero, P., Berthier, E., Kerloc'h, B., Piney, S., Felts, D., 2010. A method for the
781          assessment of the flood risk related to direct runoff and flash floods. SimHydro 2010 Sophia
782          Antipolis.
783    Reuter, H.I., Wendroth, O., Kersebaum, K.C., 2006. Optimisation of relief classification for different
784          levels of generalisation. Geomorphology 77, 79–89. doi:10.1016/j.geomorph.2006.01.001

785   Robinson, D.A., Phillips, C.P., 2001. Crust development in relation to vegetation and agricultural
786           practice on erosion susceptible, dispersive clay soils from central and southern Italy. Soil
787           Tillage Res. 60, 1–9. doi:10.1016/S0167-1987(01)00166-0
788   Schmocker-Fackel, P., Naef, F., Scherrer, S., 2007. Identifying runoff processes on the plot and
789           catchment scale. Hydrol. Earth Syst. Sci. 11, 891–906. doi:10.5194/hess-11-891-2007
790   Schumm, S.A., 1956. Evolution of drainage systems and slopes in badlands at Perth Amboy, New
791           Jersey. Geol. Soc. Am. Bull. 67, 597–646. doi:10.1130/0016-
792           7606(1956)67[597:EODSAS]2.0.CO;2
793   Smith, R.E., Goodrich, D.C., Woolhiser, D.A., Unkrich, C.L., 1995. KINEROS-A kinematic runoff and
794           erosion model. Comput. Models Watershed Hydrol. 20, 627–668.
795   Stanski, H.R., Wilson, L.J., Burrows, W.R., 1989. Survey of common verification methods in
796           meteorology. World Meteorological Organization Geneva.
797   Tetzlaff, D., Soulsby, C., Waldron, S., Malcolm, I.A., Bacon, P.J., Dunn, S.M., Lilly, A., Youngson, A.F.,
798           2007. Conceptualization of runoff processes using a geographical information system and
799           tracers in a nested mesoscale catchment. Hydrol. Process. 21, 1289–1307.
800           doi:10.1002/hyp.6309
801   Thywissen, K., 2006. Components of risk: a comparative glossary. UNU- EHS.
802   UNDHA, 1992. Internationally agreed glossary of basic terms related to disaster management. UN
803           DHA U. N. Dep. Humanit. Aff. Geneva.
804   UNDRO, 1979. Natural disasters and vulnerability analysis : report of Expert Group Meeting (No.
805           naturaldisasters00offi). Geneva.
806   Versini, P.-A., Gaume, E., Andrieu, H., 2010a. Assessment of the susceptibility of roads to flooding
807           based on geographical information - test in a flash flood prone area (the Gard region,
808           France). Nat. Hazards Earth Syst. Sci. 10, 793–803. doi:/10/793/2010/
809   Versini, P.-A., Gaume, E., Andrieu, H., 2010b. Application of a distributed hydrological model to the
810           design of a road inundation warning system for flash flood prone areas. Nat. Hazards Earth
811           Syst. Sci. 10, 805–817. doi:/10/805/2010/
812   Wischmeier, W.H., 1959. A Rainfall Erosion Index for a Universal Soil-Loss Equation. Soil Sci. Soc. Am.
813           J. 23, 246. doi:10.2136/sssaj1959.03615995002300030027x
814

**Figure captions:**

Figure 1: Scheme of the IRIP method to create the three susceptibility maps of surface runoff generation, transfer, and accumulation, with the input data

Figure 2: Description of the Lézarde catchment which is located in the Seine-Maritime County and which ranges from 1 to 138 meters of elevation with a short permanent hydrographic network

Figure 3: Description of the rainfall event of October 13, 2013 that impacted the northern part of the Lézarde catchment

Figure 4: Explanative schemes of the data formatting for the comparison with the impact databases, a) Process to detect pixel persistence and remove isolated pixels, b) presentation of the surfaces taken into account for the computation of the contingency table.

Figure 5: The IRIP map of susceptibility of the Lézarde catchment to surface runoff generation

Figure 6: The IRIP map of susceptibility of the Lézarde catchment to surface runoff transfer

Figure 7: The IRIP map of susceptibility of the Lézarde catchment to surface runoff accumulation

Figure 8: Superimposition of the high susceptibility levels of the IRIP map of accumulation and of the surface runoff regulatory zoning

Figure 9: Superimposition of the high susceptibility levels of the IRIP map of transfer and of the soil erosion regulatory zoning

Figure 10: Superimposition of the high susceptibility levels of the IRIP map of transfer and accumulation after processing and of the road network of the three sub-catchments impacted by the rainfall event, along with the road sections impacted by surface runoff and the hydraulic structure locations

Figure 11: Superimposition of the high susceptibility levels of the IRIP map of transfer and accumulation and of the soil erosion regulatory zoning

Figure 12: Photos from Google Street View illustrating the environment configuration around four impacted road sections in order to explain the reason of the IRIP false alarms

Table 1: List of the 5 indictors per map used to create the 3 IRIP maps of generation, transfer, and accumulation susceptibility, with the criteria of favourability for each indicator

Table 2: The theoretical contingency table to analyze the correlation between the IRIP maps and the comparison data

Table 3: The five verification indicators computed to analyze the correlation between the IRIP maps and the comparison data

Table 4: Result summary of the comparison between the regulatory zonings and the high susceptibility levels of the IRIP maps of transfer and accumulation, using buffer area sizes of 0, 25 and 50 meters

Table 5: Result summary of the comparison between the impact locations on the transportation network and the high susceptibility level locations on the IRIP maps of transfer and accumulation, using buffer area sizes of 25 and 50 meters
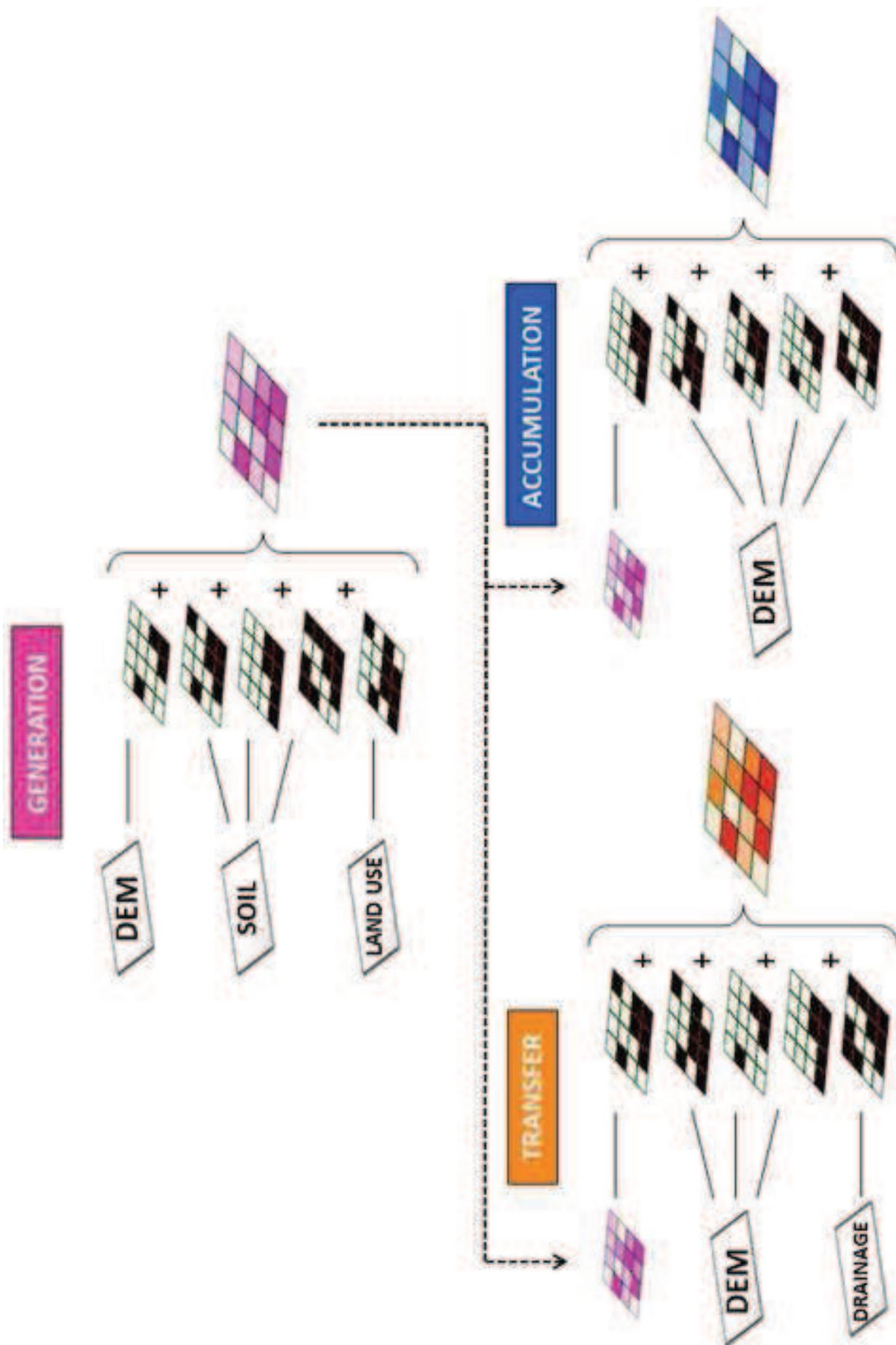
**Fig1_the_irip_method_scheme**
Click here to download high resolution image
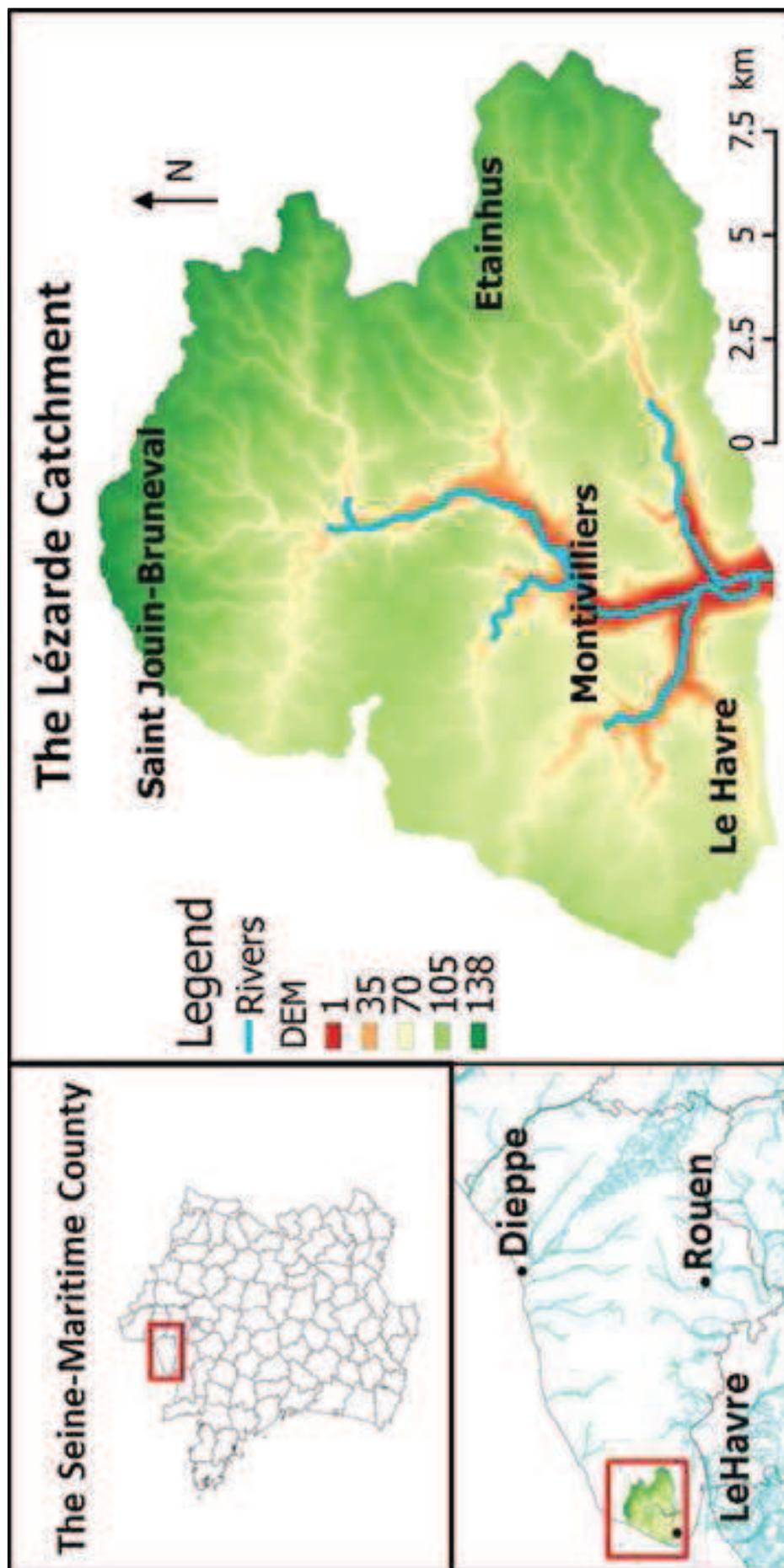
**Fig2_the_study_area**
**Click here to download high resolution image**
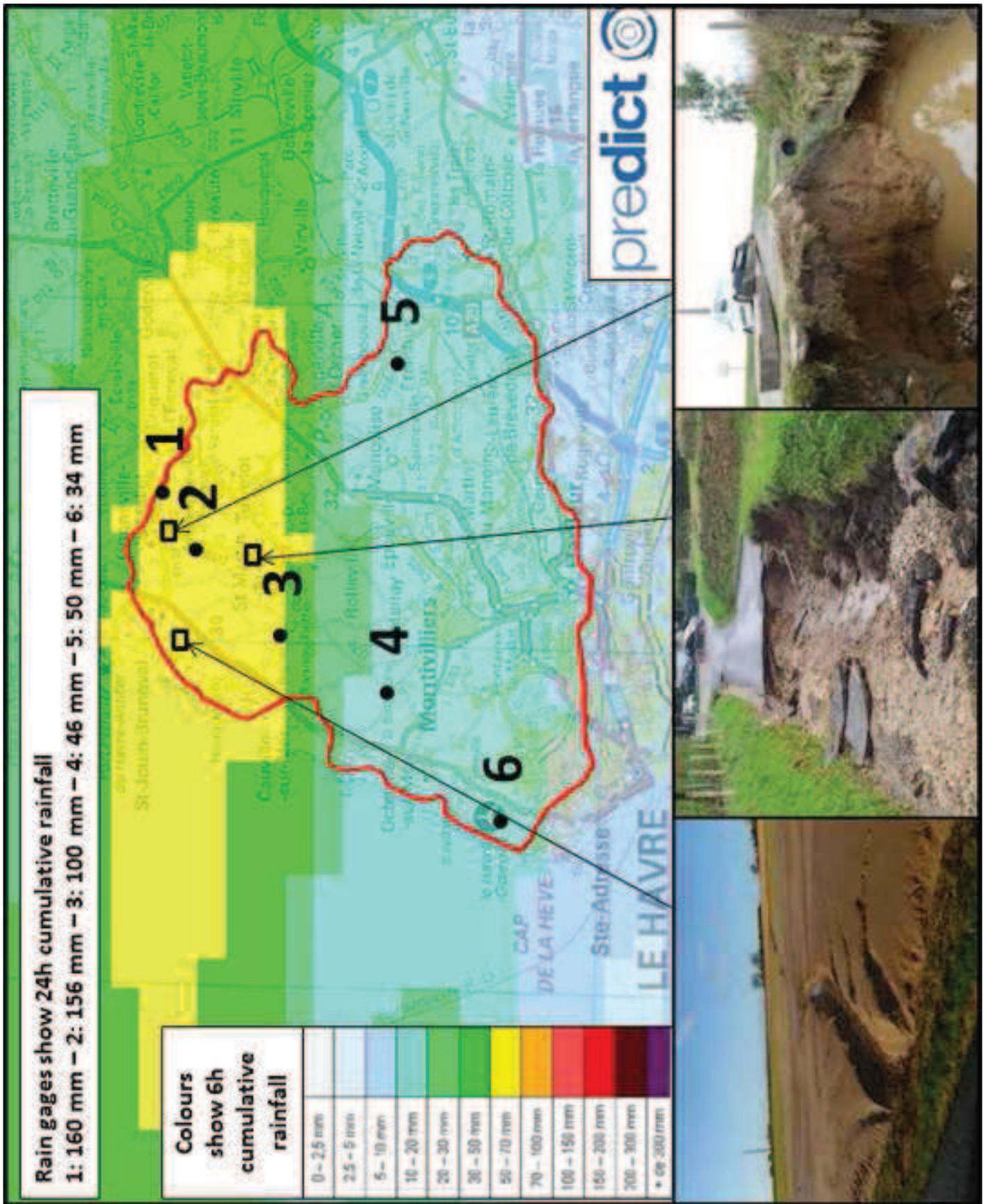
**Fig3_Rainfall_13_oct**
Click here to download high resolution image

**Fig5_IRIP_map_generation**
Click here to download high resolution image
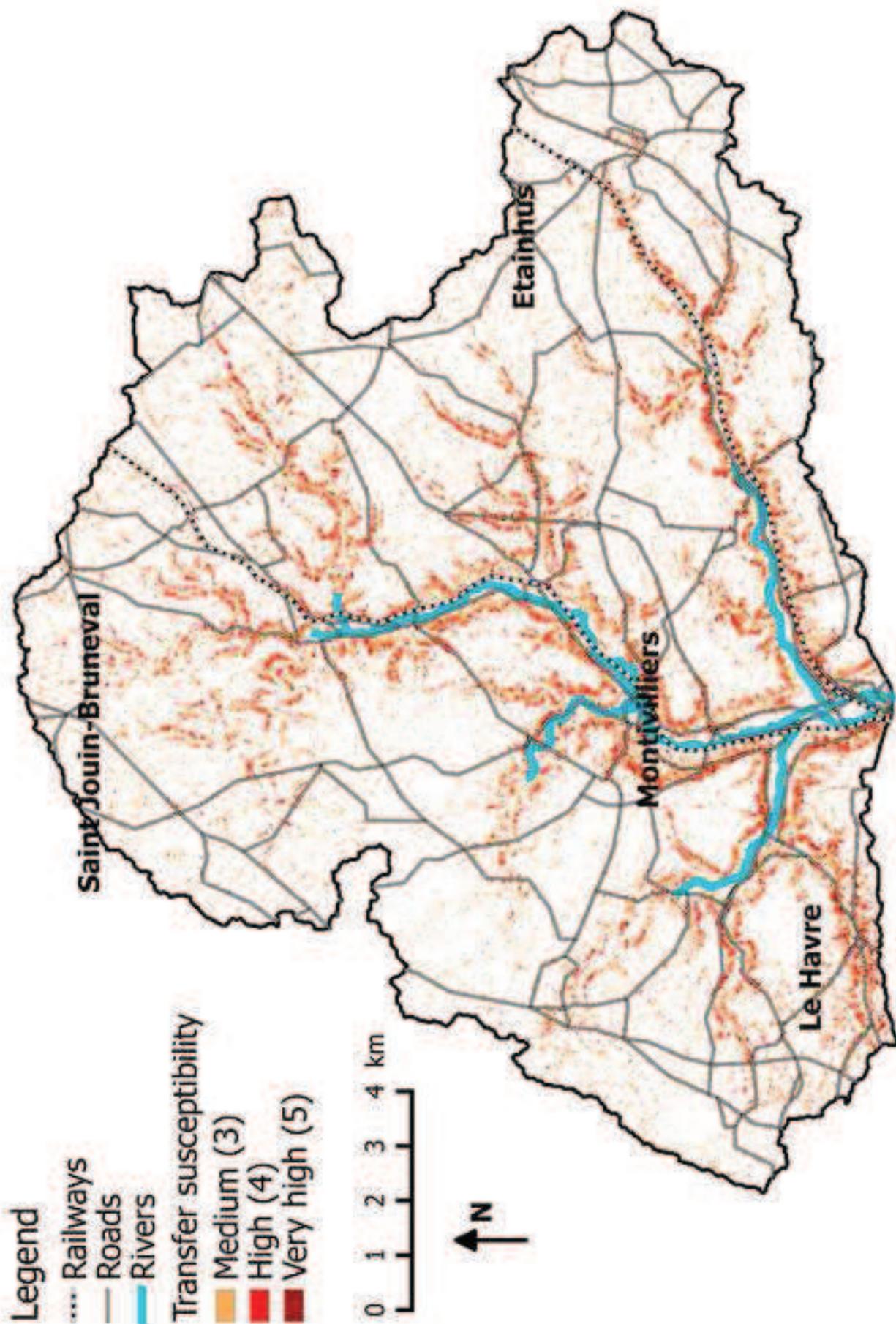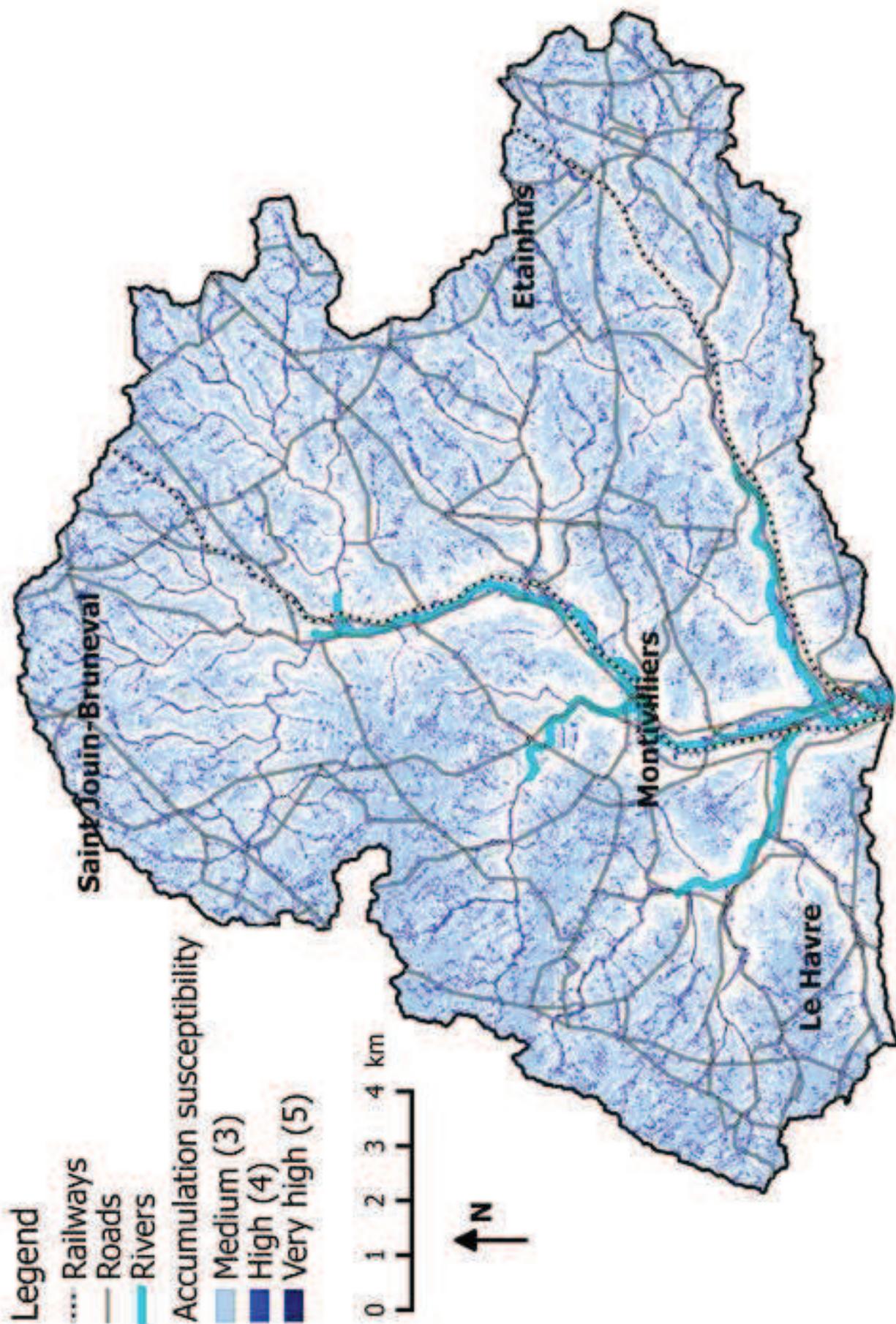
**Fig7_IRIP_map_accumulation**
**Click here to download high resolution image**



Legend

- Railways
— Roads
— Rivers

Accumulation susceptibility

Medium (3)
High (4)
Very high (5)

0  1  2  3  4 km

N

Saint Jouin-Bruneval

Etainhus

Montivilliers

Le Havre
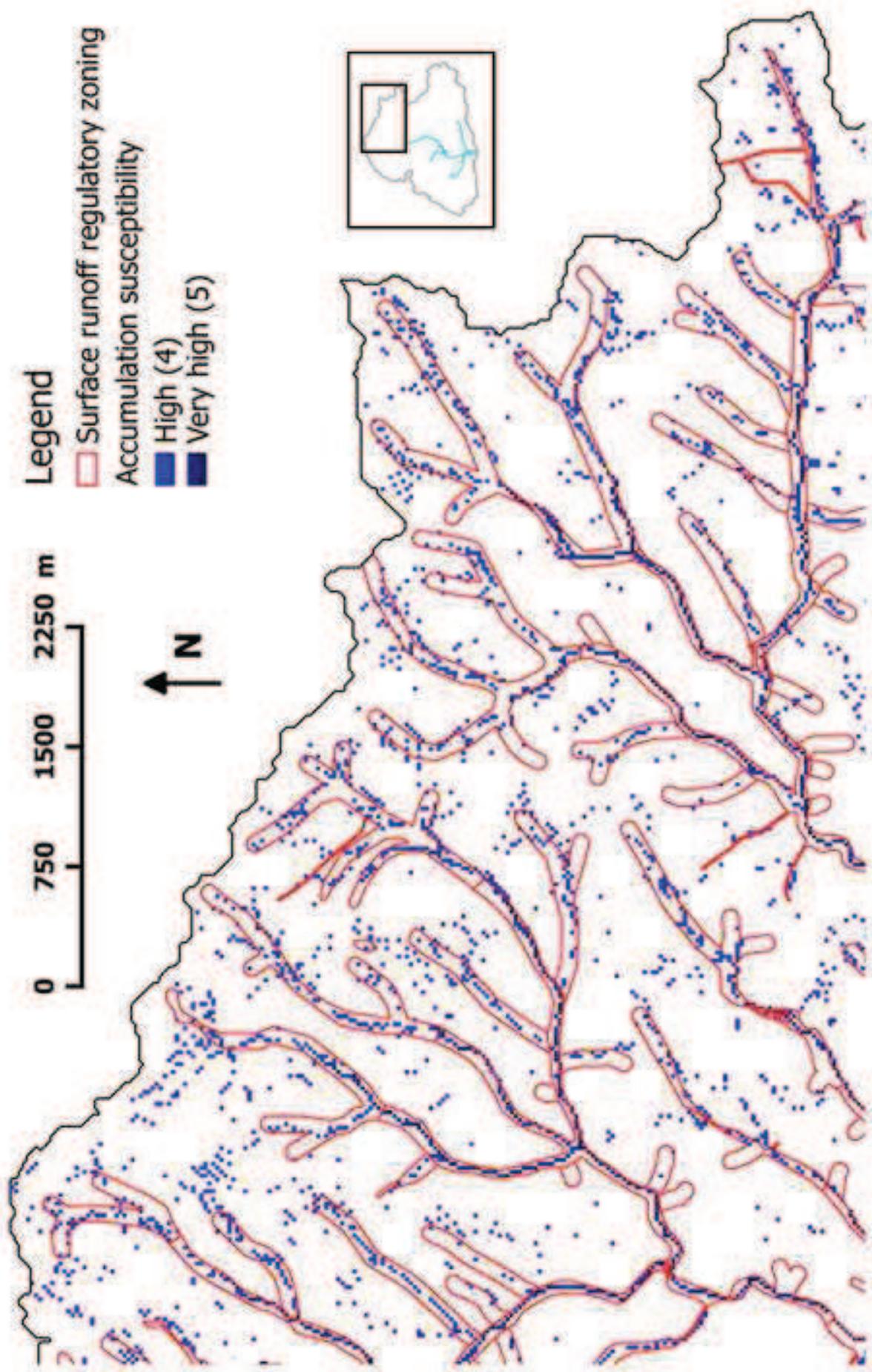
**Fig8_comparison_runoff_zoning**
Click here to download high resolution image

Legend
☐ Surface runoff regulatory zoning
Accumulation susceptibility
■ High (4)
■ Very high (5)

N

0    750    1500    2250 m
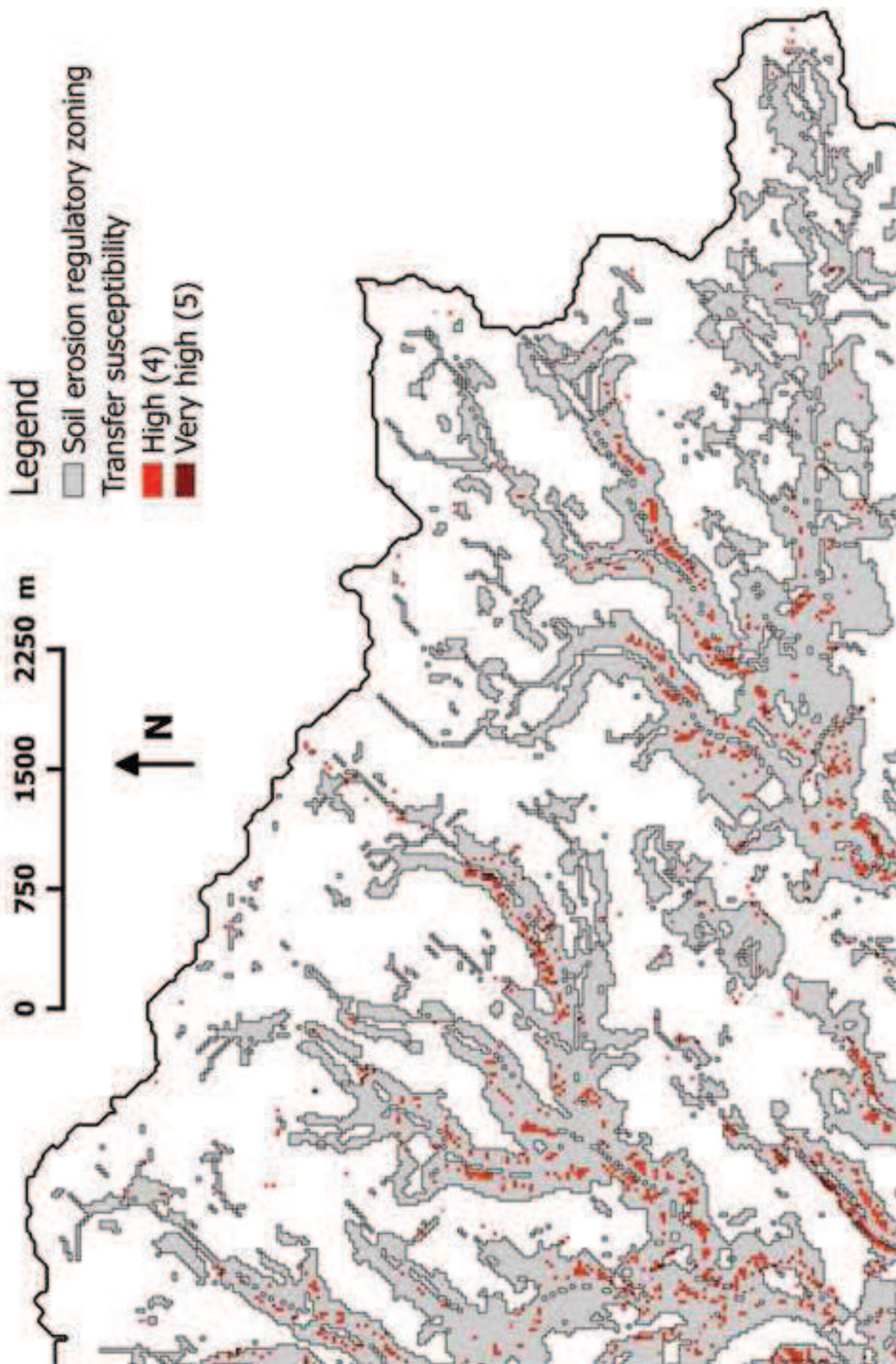
**Fig9_comparison_erosion_zoning**
Click here to download high resolution image

## Legend

Soil erosion regulatory zoning

Transfer susceptibility

High (4)

Very high (5)
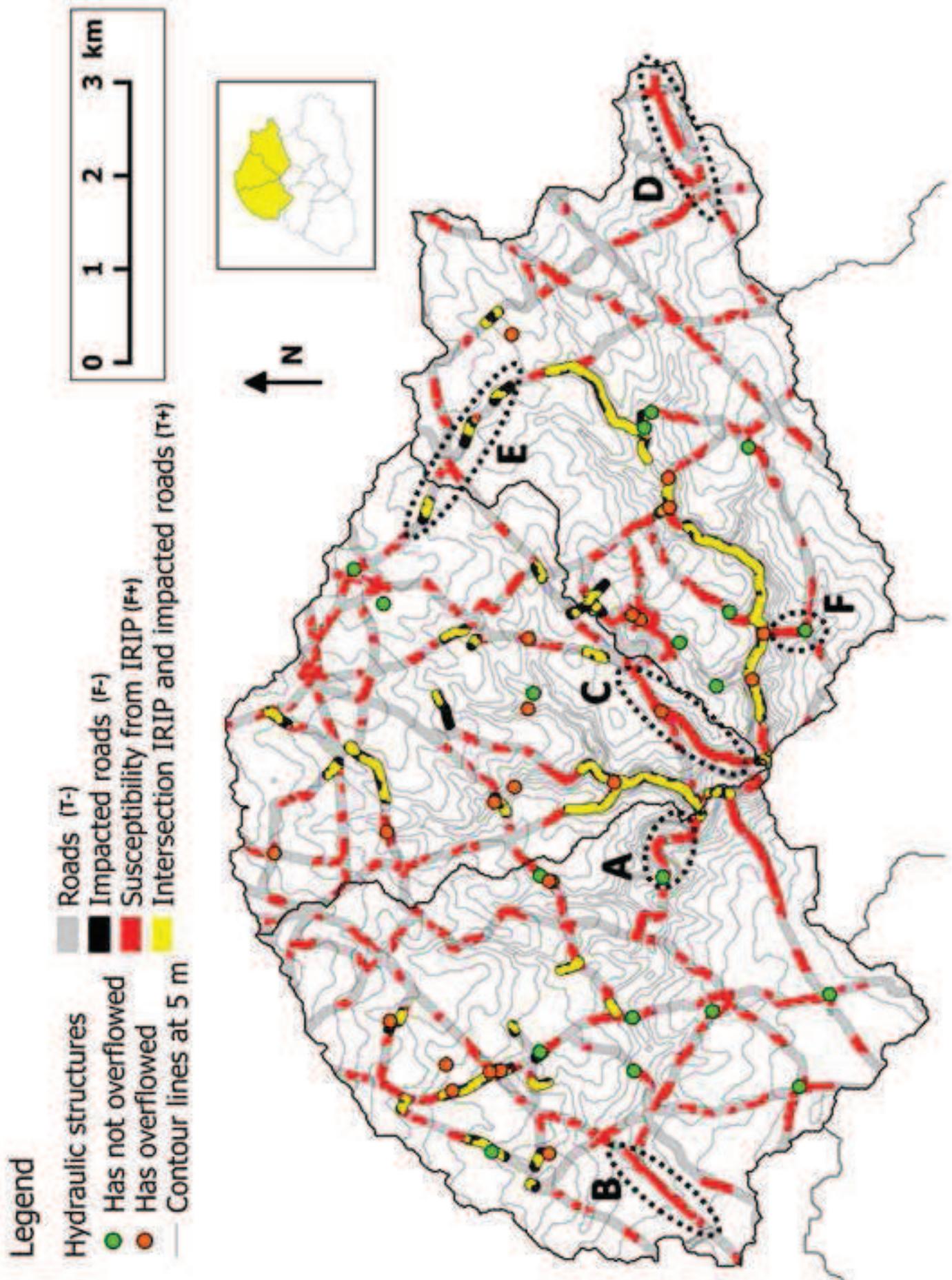
**Fig10_road_IRIP_analysis**
Click here to download high resolution image



Legend

Hydraulic structures
● Has not overflowed
● Has overflowed

Roads  (T-)
Impacted roads (F-)
Susceptibility from IRIP (F+)
Intersection IRIP and impacted roads (T+)
─ Contour lines at 5 m
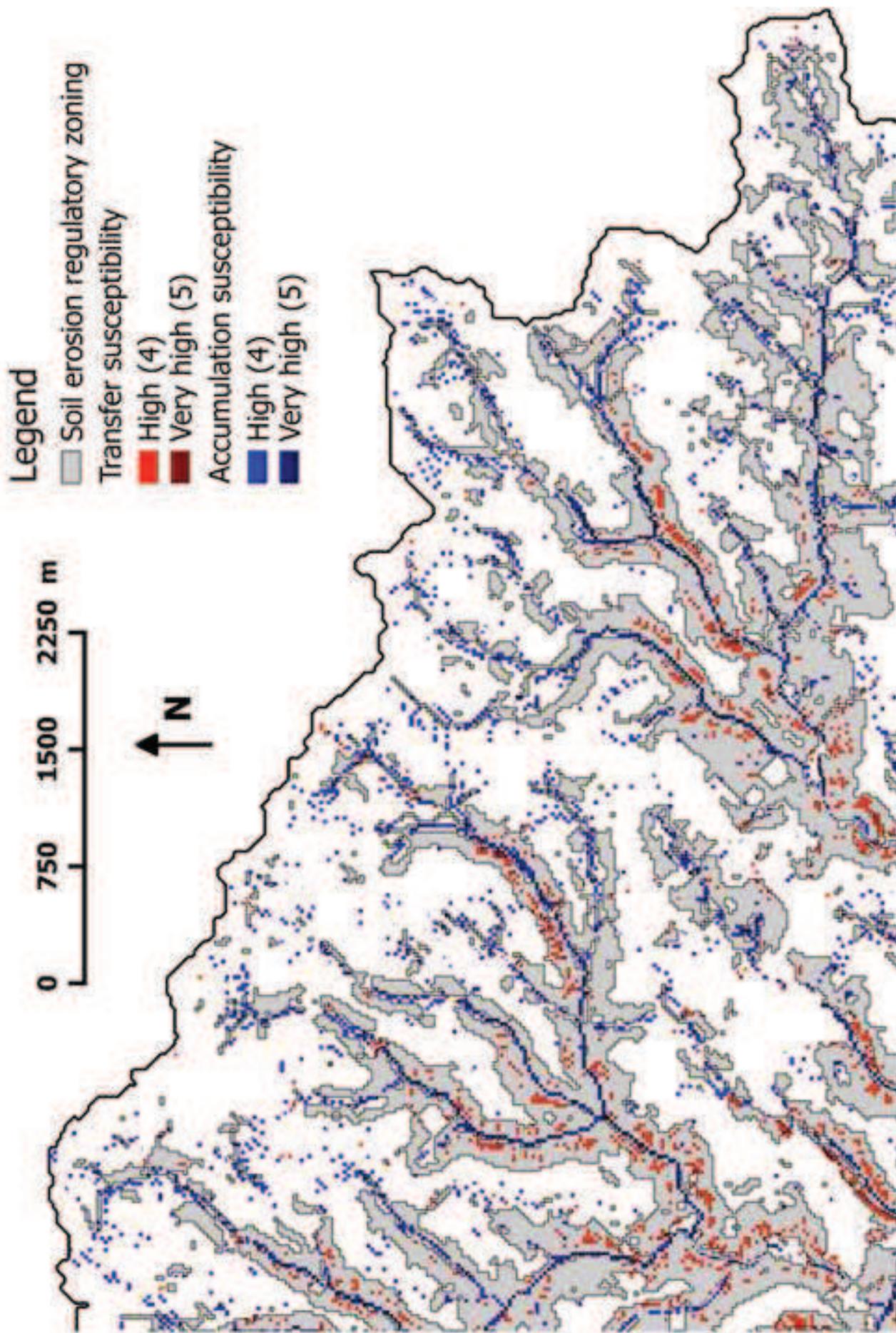
**Fig11_comparison_acc_trans_erosion_zoning**
Click here to download high resolution image

**Fig12_road_photos_vulnerability**
Click here to download high resolution image

| IRIP maps | Indicators | Values |
|---|---|---|
| Generation | Soil permeability | 0: High permeability |
| | | 1: Low permeability |
| | Soil thickness | 0: Thick soil |
| | | 1: Thin soil |
| | Soil erodibility | 0: Low erodibility |
| | | 1: High erodibility |
| | Topography | 0: Slope $< t_1$ AND topographic index $< t_2$ |
| | | 1: Slope $> t_1$ OR topographic index $> t_2$ |
| | Land use | 0: Infiltrative surfaces |
| | | 1: Impervious surfaces |
| Transfer | Upstream generation susceptibility | 0: Low upstream generation susceptibility |
| | | 1: High upstream generation susceptibility |
| | Slope | 0: Slope $< t_1$ |
| | | 1: Slope $> t_1$ |
| | Break of slope | 0: Concave break of slope |
| | | 1: Convex break of slope |
| | Catchment compacity | 0: Low Horton form factor |
| | | 1: High Horton form factor |
| | Artificial linear axes | 0: No linear axes |
| | | 1: Presence of linear axes |
| Accumulation | Upstream generation susceptibility | 0: Low upstream generation susceptibility |
| | | 1: High upstream generation susceptibility |
| | Slope | 0: Slope $> t_1$ |
| | | 1: Slope $< t_1$ |
| | Break of slope | 0: Convex break of slope |
| | | 1: Concave break of slope |
| | Topographic index | 0: Topographic index $< t_2$ |
| | | 1: Topographic index $> t_2$ |
| | Flow accumulation | 0: Low flow accumulation |
| | | 1: High flow accumulation |

| | | Observed event | | |
|---|---|---|---|---|
| | | Yes | No | Total |
| IRIP | Yes | True positives | False positives | Forecast yes |
| | No | False negatives | True negatives | Forecast no |
| | Total | Observed yes | Observed no | Total |

**Table3_the_five_verification_indicators**

| Verification indicators | Formulas | Interpretation |
|---|---|---|
| Accuracy | $\dfrac{True\ positives + True\ negatives}{Total}$ | Range: 0 to 1 <br> Perfect score: 1 |
| Bias | $\dfrac{True\ positives + False\ positives}{True\ positives + False\ negatives}$ | Range: 0 to ∞ <br> Perfect score: 1 <br> <1 underforecast, >1 overforecast |
| Success ratio | $\dfrac{True\ positives}{True\ positives + False\ positives}$ | Range: 0 to 1 <br> Perfect score: 1 |
| Probability of detection | $\dfrac{True\ positives}{True\ positives + False\ negatives}$ | Range: 0 to 1 <br> Perfect score: 1 |
| False alarm ratio | $\dfrac{False\ positives}{True\ positives + False\ positives}$ | Range: 0 to 1 <br> Perfect score: 0 |

| IRIP pixels | Verification indicators | Surface runoff zoning / Map of accumulation | | | Soil erosion zoning / Map of transfer | | |
|---|---|---|---|---|---|---|---|
| | | 0 m | 25 m | 50 m | 0 m | 25 m | 50 m |
| ≥4 | Accuracy | 0.84 | 0.76 | 0.68 | 0.69 | 0.51 | 0.39 |
| | Bias | 0.41 | 0.25 | 0.18 | 0.12 | 0.07 | 0.06 |
| | Success ratio | 0.41 | 0.53 | 0.59 | 0.64 | 0.82 | 0.91 |
| =5 | Accuracy | 0.86 | 0.77 | 0.68 | 0.68 | 0.48 | 0.36 |
| | Bias | 0.06 | 0.04 | 0.03 | 0.01 | 0.00 | 0.00 |
| | Success ratio | 0.72 | 0.89 | 0.92 | 0.55 | 0.84 | 0.92 |

| Verification indicators | Impacts on the transportation network / Maps of transfer and accumulation | | | |
|---|---|---|---|---|
| | Roads | | Railways | |
| | 25 m | 50 m | 25 m | 50 m |
| Accuracy | 0.68 | 0.65 | 0.34 | 0.30 |
| Bias | 3.22 | 3.10 | 9.58 | 7.73 |
| Success ratio | 0.23 | 0.23 | 0.08 | 0.12 |
| Probability of detection | 0.73 | 0.72 | 0.80 | 0.90 |
| False alarm ratio | 0.77 | 0.77 | 0.92 | 0.88 |